Geologic stability of Mystic Lake dam, Gallatin County, Montana, and computer simulation of potential flood hazards from the failure of the dam
by Graham Stephen Hayes

A thesis submitted in partial fuIIfiIlment of the requirements for the degree of MASTER OF SCIENCE i n Earth Science
Montana State University

Abstract:
The failure of Mystic Lake dam poses a major threat to the residents of the Bozeman Creek drainage. Outdated engineering practices used in the construction of the dam coupled with an unstable geologic setting create a potentially hazardous situation. The east abutment of the oam is founded in the toe of a Quaternary landslide. Water seeps through the landslide debris and ponds in a depression at the foot of the dam. Unvegetated slumo scarps in the landslide directly below the dam site are attributed to the increased pore pressure from the seepage water. The potential for liquefaction in the event of an earthquake is extrerne Iy high.

A mathematical model is programmed in FORTRAN IV to simulate the failure of the dam and the movement of the floodwave. The hypothetical failure is induced by overtopping the dam with a rain-storm discharge greater than the spillway capacity (780 cfs). The breach is assumed to erode as an exponential function of time, producing an estimated peak discharge of 83,500 cfs in approximately 7.5 minutes.

A hydraulic routing method utilizing the complete equations of unsteady flow is solved numerically by a four-point implicit finite difference method.

Changes in the flow regime of Bozeman Creek make the computation of the initial water surface profile and the establishment of intermediate boundary conditions impossible. Until sufficient gaging data are available# trie routing portion of the model is not applicable to Bozeman Creek and the extent of flooding from the failure of Mystic Lake dam cannot be simulated.

An estimate for the extent of flooding from the failure of the dam is approximated by plotting the percentage attenuation of the breach hydrograph against the depth of flow.

A 60 percent attenuation yields a depth' of flow of 10.5 feet, at the canyon mouth # 4.5 feet deeper than the 5 CO year flood.

STATEMENT OF PERMISSION TO COPY

In presenting this thesis in partial fullfillment of the requirements for an advanced degree at Montana State University, I agree that the Library shall make it freely available for inspection. I further agree that permission for extensive copying of the thesis for scholarly purposes may be granted by my major professor, or, in his absence, by the Director of Libraries. It is understood that any copying or publication of this thesis for financial gain shall not be allowed without written permission.

Signature Andrea Hayes

Date April 10, 1981

GEOLOGIC STABILITY OF MYSTIC LAKE DAM, GALLATIN COUNTY, MONTANA, AND COMPUTER SIMULATION OF POTENTIAL FLOOD HAZARDS FROM THE FAILURE OF THE DAM

by

GRAHAM STEPHEN HAYES

A thesis submitted in partial fullfillment
of the requirements for the degree

of

MASTER OF SCIENCE

in

Earth Science

Approved:

Chairman, Graduate Committee

Head, Major Department

Graduate Dean

MONTANA STATE UNIVERSITY
Bozeman, Montana

April, 1981

VITA

Graham Stephen Hayes was born in Chatham, Ontario, Canada on December 28, 1955. His parents are Wilfred H. Hayes and Katherine V. Hayes. He graduated from Cypress Lake Senior High School, Fort Myers, Florida, in June 1973. He received a Bachelor of Science degree in geology from Wheaton College, Wheaton, Illinois, in June 1977. After working one summer for the Geological Survey of Canada, he married Karen S. Markello on June 17, 1978. He entered the graduate school at Montana State University the following September, and held both research and teaching assitantships while working toward a Master of Science Degree in Earth Sciences.

ACKNOWLEDGMENT

The author wishes to extend his thanks to Dr. Stephan Custer (committee chairman), and Dr. Donald L. Smith (reading committee), for initiating the study and providing continual encouragement and help throughout the investigation. Special thanks to Dr. Michael Amein, Univ. of North Carolina Raleigh, for his helpful correspondence and program listings. My appreciation to Professor Martin Faulkner and Dr. Del Dyreson (reading committee), and to Mark Hinrichs and Georgia Ziemba for their invaluable help with the programming aspect of the thesis.

The writer is also indebted to Mr. Norm Buhl, of the U.S. Forest Service, for allowing vehicle access to the dam site; to Mr. Ralph Bergantine, of the U.S. Soil Conservation Service, for providing stream cross-section data; to Professor Robert Taylor and Glen Wyatt for their advice concerning drafting problems; and to Tom Grady for the countless hours of discussion and head-scratching concerning the equations of unsteady flow.

Finally, a note of thanks to my wife Karen, for her constant support, patience with my long and late hours on the computer, and for typing the final copy of the thesis.

TABLE OF CONTENTS

LIST OF FIGURES

ABSTRACT

The failure of Mystic Lake dam poses a major threat to the residents of the Bozeman Creek drainage. Outdated engineering practices used in the construction of the dam coupled with an unstable geologic setting create a potentially hazardous situation. The east abutment of the dam is founded in the toe of a Quaternary landslide. Water seeps through the landslide debris and ponds in a depression at the foot of the dam. Unvegetated slump scarps in the landslide directly below the dam site are attributed to the increased pore pressure from the seepage water. The potential for liquefaction in the event of an earthquake is extremely high.

A mathematical model is programmed in FORTRAN IV to simulate the failure of the dam and the movement of the floodwave. The hypothetical failure is induced by overtopping the dam with a rain-storm discharge greater than the spillway capacity (780 cfs). The breach is assumed to erode as an exponential function of time, producing an estimated peak discharge of 83,500 cfs in approximately 7.5 minutes. A hydraulic routing method utilizing the complete equations of unsteady flow is solved numerically by a four-point implicit finite difference method.

Changes in the flow regime of Bozeman Creek make the computation of the initial water surface profile and the establishment of intermediate boundary conditions impossible. Until sufficient gaging data are available, the routing portion of the model is not applicable to Bozeman Creek and the extent of flooding from the failure of Mystic Lake dam cannot be simulated.

An estimate for the extent of flooding from the failure of the dam is approximated by plotting the percentage attenuation of the breach hydrograph against the depth of flow. A 60 percent attenuation yields a depth of flow of 10.5 feet at the canyon mouth, 4.5 feet deeper than the 500 year flood.

INTRODUCTION

Location

Bozeman Creek drains 52.4 square miles on the northern flanks of the Gallatin Range, southwestern Montana. The upper 4.9 square miles of the drainage basin drain into Mystic Lake (Fig. 1). The lake is 12 miles southeast of Bozeman in the eastern half of section 25, Township 3 South, Range 6 East, and in the western half of section 30, Township 3 South, Range 7 East. From Mystic Lake, Bozeman Creek flows 7 miles through a narrow, forested, northwest-trending canyon (Fig. 1). The lower reach of the stream, between the canyon mouth and the East Gallatin River, occupies a narrow floodplain (less than one mile wide), which is undergoing steady urbanization. Many residential and commercial developments have established on the floodplain including part of downtown Bozeman (Fig. 1).

Purpose of the Study

According to guidelines established by the U.S. Corps of Engineers (1975), Mystic Lake dam is classified as having a high downstream hazard potential. In an executive summary Foster (CH2M Hill, 1980, p. iv) stated:

> Based on visual reconnaissance and engineering judgement, the dam is located such that its failure could cause extensive property damage and possible loss of life.

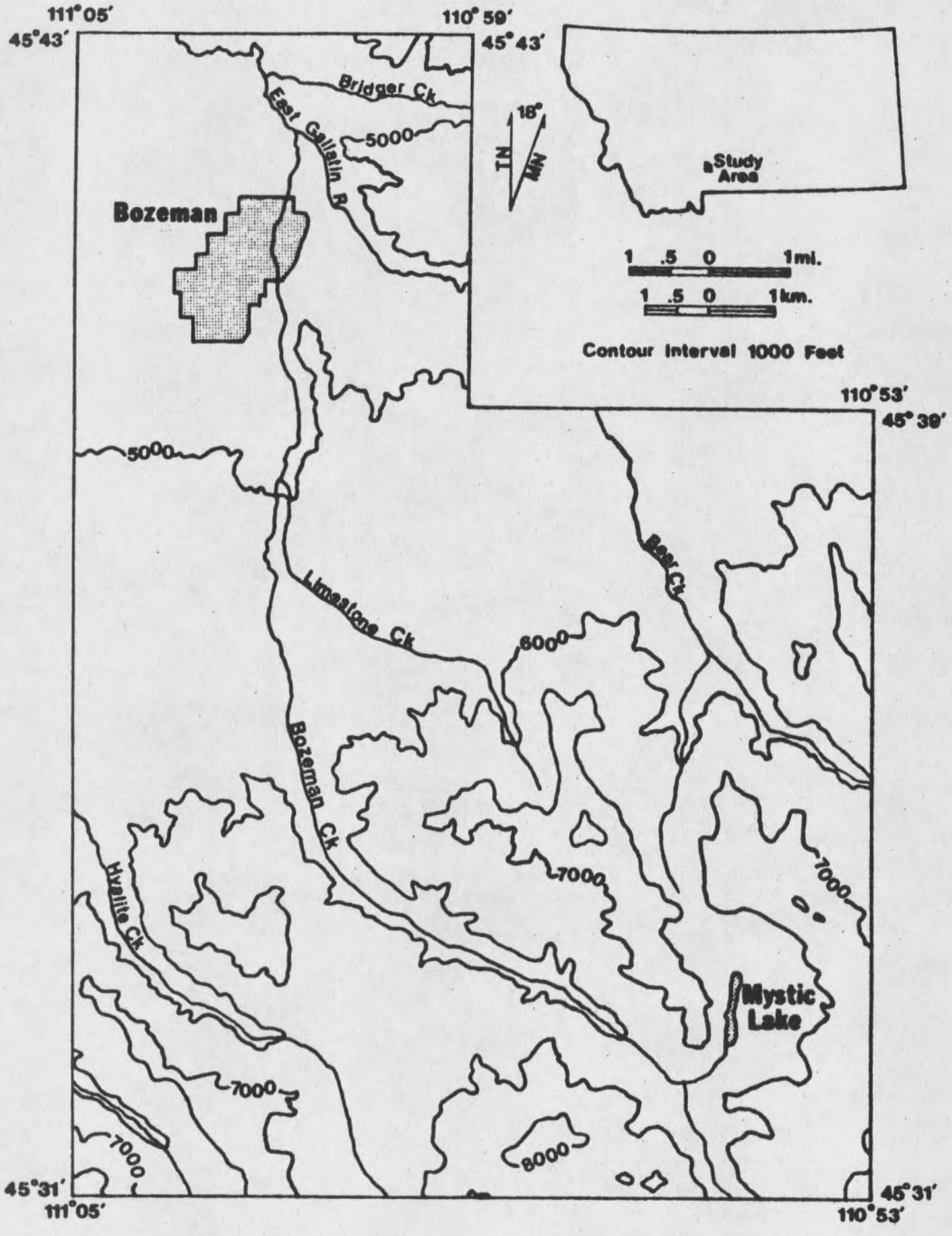

Figure 1. Location map. Note the spatial relationship between Mystic Lake, Bozeman Creek and the town of Bozeman.

In his recommendations to the city of Bozeman, the Bozeman Creek Reservoir Company and the U.S. Corps of Engineers, he stressed the need for further evaluation of the dam's geologic stability and for a hydraulic routing to establish the extent of downstream flooding associated with the failure of the dam.

The purpose of this investigation is twofold: first, to evaluate the stability of Mystic Lake dam by compiling all available engineering data and conducting a geologic investigation of the dam site, and second, to demonstrate the extent of potential flooding along Bozeman Creek by numerically simulating the failure of the dam and the movement of the floodwave downstream.

History of the Dam

The following section was summarized from a report by Bozeman City Engineer, Art Van't Hul (1980).

Mystic Lake dam was constructed in 1903 and 1904 on U.S. Forest Service property through a special use permit granted to the city of Bozeman and the Bozeman Creek Reservoir Company. The lake is used to store irrigation and municipal waters. The original earth-fill structure measured 43 feet in height from the outlet pipes (one 16 and the other 12 inches in diameter), to the dam crest (Fig. 2-A,B). Both

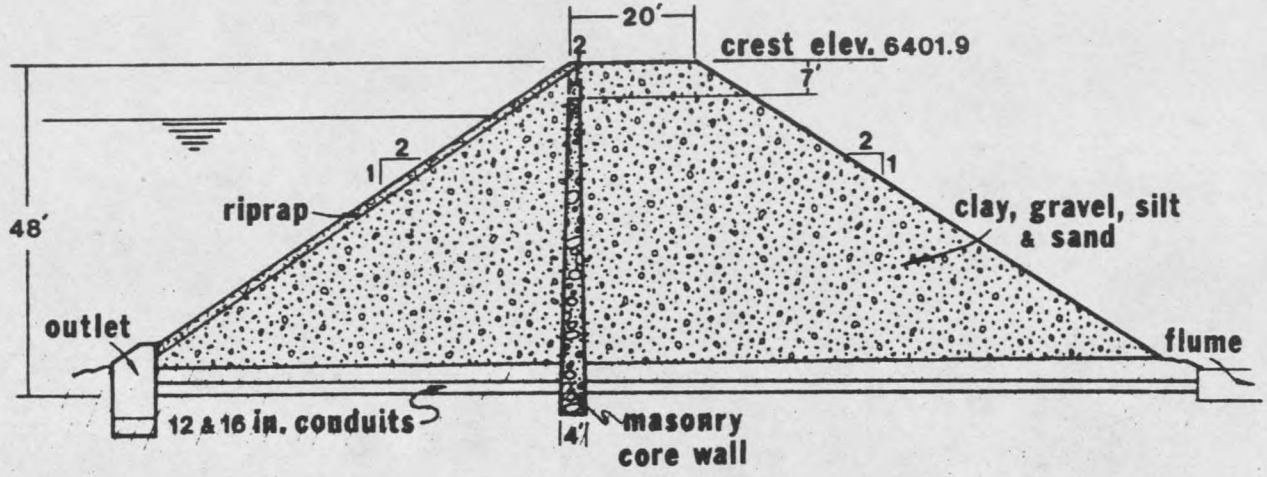

A. Cross Section

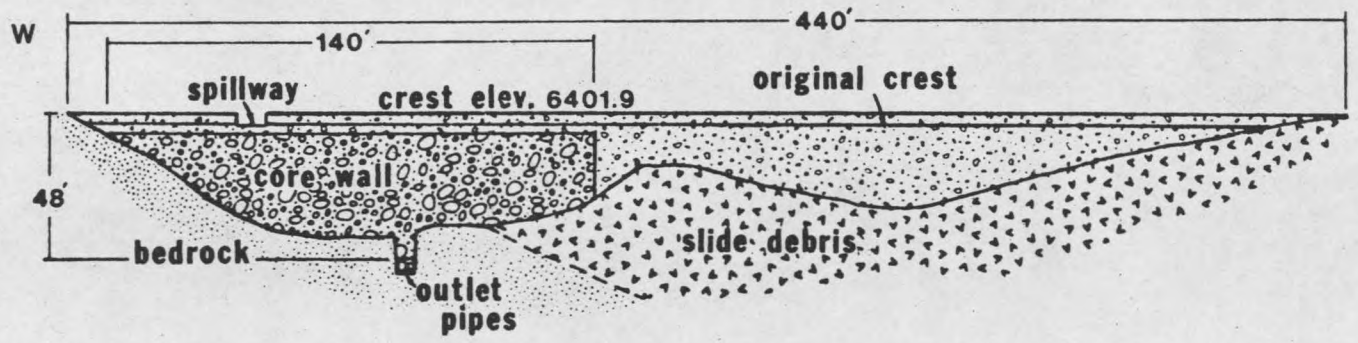

B. Profile - Longitudinal

Figure 2. Engineering drawings of Mystic Lake dam. Cross-section A is drawn through the dam along the outlet pipes. Note the extent of the core wall in the longitudinal profile B. Where the core wall is absent, seepage water ponds in a depression at the toe of the dam, plan view C.

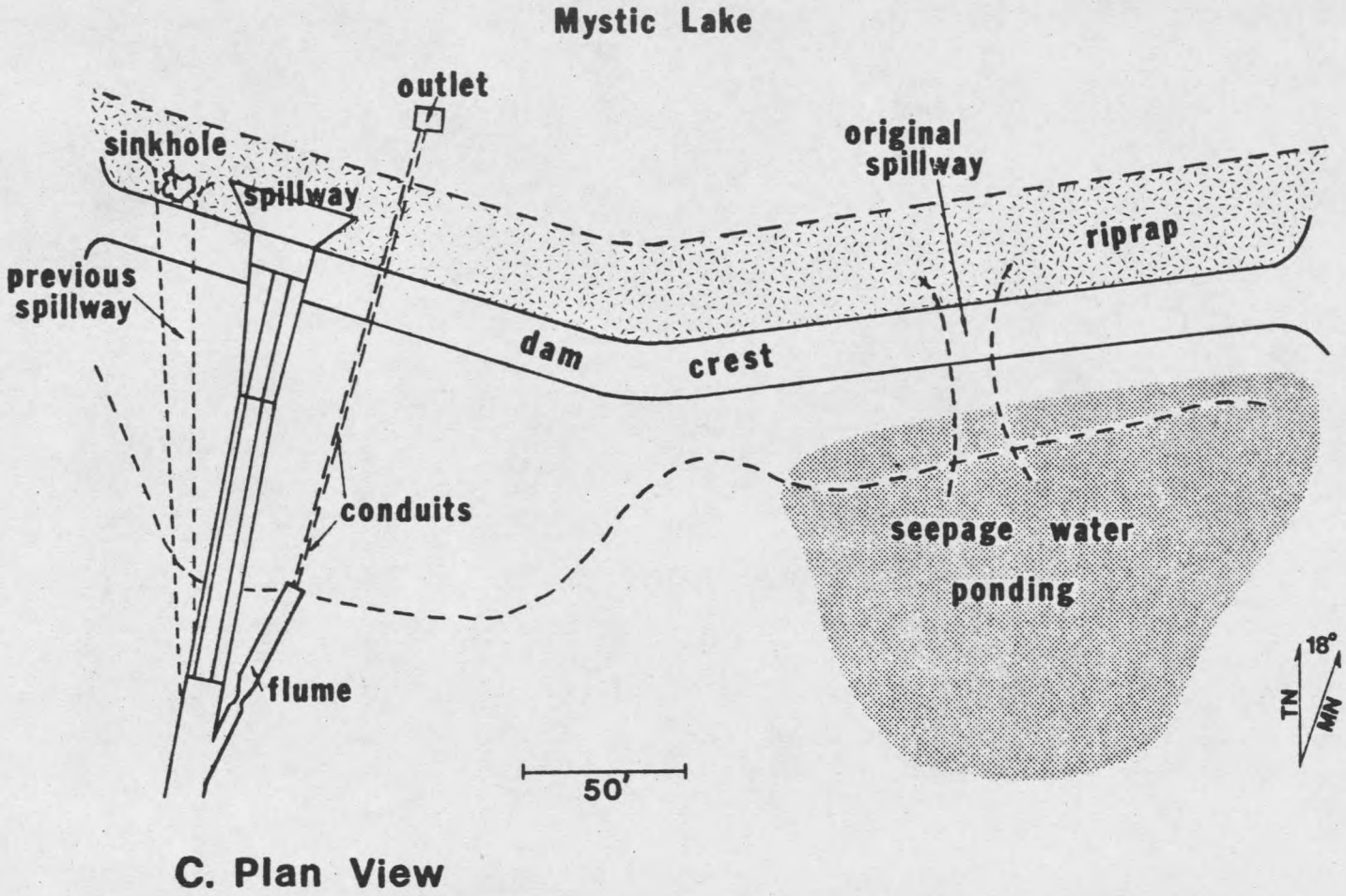

C. Plan View

Figure 2. (continued)

upstream and downstream faces had slopes of 2 to 1 with the upstream face riprapped. A masonry core wall, 4 feet thick at the base, 2 feet thick at the top, and 140 feet long, extended from the west abutment through the center line of the dam. The top of the core wall was approximately 2 feet below the original crest of the dam (Fig. 2-A, B).

There have been several modifications to the dam since its installation in 1903. A concrete spillway was constructed in 1919 near the west abutment to replace the original timber spillway (Fig. 2-C). In 1932, a high runoff event leaving only a .9 foot freeboard on the dam, prompted officials to raise the dam crest by 3 feet to the height of the spillway cover slab. In 1959, a new concrete spillway, 185 feet long and 20 feet wide was installed with a Parshall Flume at the outlet pipes (Fig. 2-C). At the same time, the dam crest was raised two feet to its present height of 48 feet. At this new elevation, the 440 foot long dam impounded 1190 acre-feet at the spillway crest, and 1520 acre-feet at the dam crest. In the fall of 1964, the old gate structure was dismantled and a new concrete outlet control with a hand operated slide gate was installed. Three years later, in 1967, a longitudinal crack developed in the lower end of the spillway floor. The repairs were made by injecting a

mixture of masonry cement, washed sand, and bentonite into a series of holes drilled through the spillway floor.

In July, 1977, water was observed entering a sinkhole in the upstream face of the dam (Fig. 2-C), accompanied by a loud roar from within the dam. Muddy water and algae were observed issuing from a pool 200 to 300 feet downstream from the end of the spillway. As the reservoir level decreased, the sound from within the dam lessened and the flow of water through the sinkhole diminished (Williams, 1977). Drill hole and fluorescein dye tests conducted by Northern Testing Laboratories (1977), and television monitoring of the outlet pipes by Bozeman city officials in 1977-78, led to the conclusion that differential settlement of the core wall and the dam embankment had sheared the 12 inch outlet pipe. Inspections revealed that the 12 inch diameter pipe had a 3 inch vertical displacement at the upstream face of the core wall, and that both cast iron conduits had long bends and locally out-of-round sections. In order to prevent further removal of material from the dam by piping, and additional sinkhole development, mechanical expanding plugs were inserted into the upstream and downstream ends of the 12 inch outlet pipe as a temporary measure until more complete repairs could be made (Northern Testing Laboratories, 1977).

It was recommended that both outlet pipes be reshaped, lined and grouted and that a grout curtain be applied to the upstream face of the core wall (Northern Testing Laboratories, 1977; Williams, 1977). To this date, final repairs have not been undertaken. AS OF APR 1 1981

Dam Site Geology

To summarize the geologic history of the region, compressive forces of the Laramide orogeny deformed the rocks in the Mystic Lake area into a series of northwest-trending folds, 50-60 million years ago. At the culmination of the compressive phase, thrust faults developed, displacing rock units horizontally and vertically. Normal faults evolved as these forces diminished (McMannis, 1955; Aram, 1979; Hughes, 1980). 50 million years ago, after a period of erosion and stream development, extensive andesite flows and breccias covered the north end of the Gallatin Range (Chadwick, 1970). Further erosion produced the present topography. A landslide involving the volcanic breccias flowed from the east and formed a natural dam at the southern end of Mystic Lake over 150 years ago (tree ring count).

A generalized geologic map was produced for the purposes of this study (Fig. 3). The rock units mapped by Roberts (1964a; 1964b) were lumped into undifferentiated

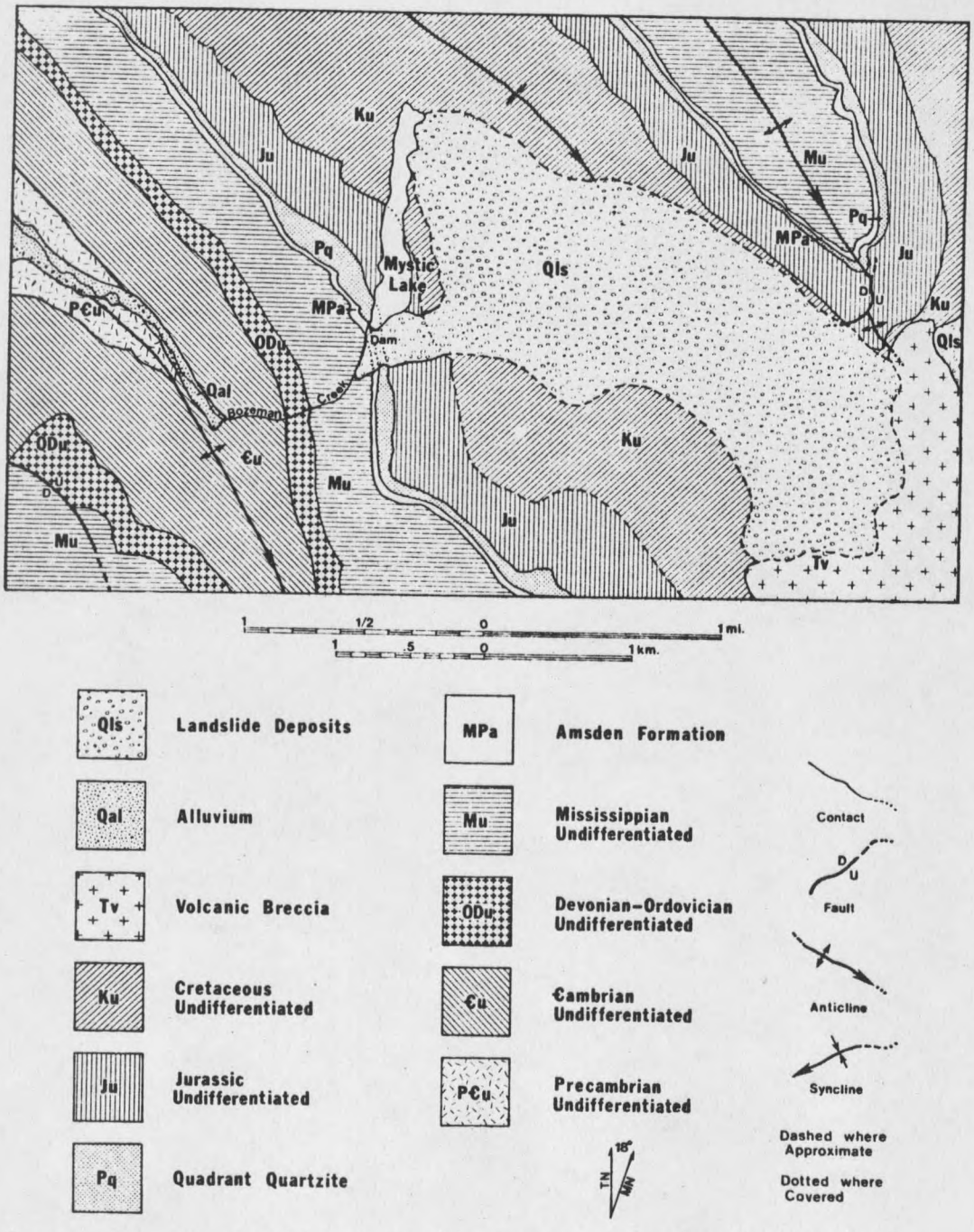

Figure 3. Generalized geologic map of the Mystic Lake region. The dam is founded in the upper dolomite of the Amsden Formation, the Quadrant Quartzite and a Quaternary landslide deposit. (After Roberts, 1964a; 1964b).

units with age distinction only. Three units which act as the foundation of the dam, the Amsden Formation, Quadrant Quartzite and the landslide deposit, retain the original status assigned by Roberts. The volcanic breccia was also mapped separately as it is the source rock for the landslide debris.

A field check of the dam site showed that Roberts (1964b) incorrectly mapped portions of the Jurassic Morrison and the Cretaceous Kootenai Formations as part of the Quaternary landslide deposit along the eastern shore of Mystic Lake. Outcrops of the carbonaceous shale of the upper Morrison, basal conglomerate and gastropod rich lacustrine limestones of the Kootenai support this conclusion. The contact at the toe of the slide, downstream from the dam was also mapped in error. The contact was extended south to the the first stream confluence where Paleozoic rocks are exposed.

The dam site is located on the northeast limb of an anticline that plunges to the southeast (Fig. 3). The upper portion of the Amsden Formation, which underlies 10-15 percent of the west abutment, is a resistant, fine-grained, white to buff dolomite with interbedded stringers of yellowish white, medium-grained, quartzose and calcareous

sandstones. According to McMannis (1955), the contact between the Amsden and the Quadrant is gradational. The boundary is drawn where the section becomes dominantely sandstone. Both units strike N 30° W and dip 50° NE. The Quadrant Quartzite makes up 25 percent of the foundation. Elsewhere the Quadrant is a resistant cliff forming unit, but at the dam it is a friable, medium grained, buff, quartz sandstone held together by calcareous cement. The remainder of the dam is founded in the toe of the landslide deposit. The grain sizes within the deposit range from boulder size angular blocks to silt size particles derived from the andesite breccia. The breccia has a blocky texture and imparts a distinctive rust coloration to the landslide deposit.

PROBLEMS ASSOCIATED WITH THE DAM

With the exception of the failure of the outlet pipe, Mystic Lake dam has functioned relatively well for the last 76 years. Nevertheless, there are many problems associated with the dam. When viewed singly these problems do not appear significant; however, when presented as a composite of interrelated problems they warrant careful consideration. The problems will be discussed in three sections; engineering and construction, geologic stability and downstream flood hazards.

Engineering and Construction

Building an earth dam with a core wall is no longer considered to be a safe engineering practice (Williams, 1959; Sowers, 1962). In fact, one has to look back twenty years into the literature to even find mention of a masonry core wall. Originally, the core wall was thought to be the principal means of reducing the flow of water through the dam as well as providing additional structural strength. However, a core wall even 2 to 3 feet thick can not withstand the pressures exerted on the dam (Williams, 1959). Williams (1959, p. 4) also reported that:

> In the case of Mystic Lake, the core wall is known to have cracked before construction was completed. The extent of cracking is not known . . . however, the core wall must be discounted as far

as imparting any structural strength.

The "additional strength" provided by the core wall prompted the engineers of Mystic Lake dam to build the embankment slopes at a much steeper angle (2:1) than allowed by modern safety requirements (Williams, 1959). Furthermore, the core wall does not extend the total length or height of the dam (Fig. 2-B). Where the core wall is absent near the east abutment, a seepage problem exists. Water moves through the dam at a rate which varies with the reservoir level and accumulates in a depression immediately downstream from the dam (Fig. 2-C) (Williams, 1959; Northern Testing Laboratories, 1977; CH2M Hill, 1980). It is feared that water ponding in such a way will raise the pore-water pressure in the foundation and embankment material and lead to the failure of the dam (CH2M Hill, 1980).

Part of the seepage problem may also be due to the lack of "zonation" of the embankment materials (Williams, 1959). A properly constructed earth dam should be built up in zones with the least permeable material at the core and layers of progressively more permeable material built out to the dam face (Williams, 1959; U.S. Bureau of Reclamation, 1974; Barron, 1977; Wilson and Marsal, 1979). Drill cores and seepage tests conducted by Northern Testing Laboratories

revealed "permeable lenses or internal erosion channels" within the embankment materials of Mystic Lake dam (Northern Testing Laboratories, 1977).

The failure of the outlet pipes and the resulting sinkhole development is attributed to the differential settlement of the dam. If the settlement continues, subsequent breakage of the outlet pipes will continue and may lead to the failure of the dam (Northern Testing Laboratories, 1977; Williams, 1977; CH2M Hill, 1980).

Overtopping of the dam or spillway by unusually high storm events is the second most common cause of dam failures in the U.S. (Middlebrooks, 1953; Fread and Harbaugh, 1973; Wilson and Marsal, 1979). In conducting a study on Mystic Lake dam, CH2M Hill (1980) estimated and routed a probable maximum flood (PMF) through the reservoir. A PMF is the largest flood that can reasonably be expected from a combination of the most severe hydrologic and meteorologic conditions possible in a given region (Chow, 1964; U.S. Bureau of Reclamation, 1977; CH2M Hill, 1980). The precipitation in the 4.9 square mile drainage basin was estimated to be 11.8 inches in 6 hours, 15.7 inches in 12 hours, and 18.1 inches in 72 hours. It was assumed that the rain fell on snowpack and that the contribution of snowmelt to runoff was equal to

the rate of infiltration. The resulting PMF had an estimated volume of 5,600 acre-feet and a peak discharge of 36,800 cfs. Because the spillway on the dam has a maximum capacity of 780 cfs, the dam would be overtopped after approximately 23 percent of the PMF had entered the reservoir (CH2M Hill, 1980).

In rechecking CH2M Hill's figures against data contained in the U.S. Bureau of Reclamation, "Design of Small Dams" (1977), the PMF in this area should produce only 14.5 inches of rain in 72 hours; a volume difference of 1,820 acre-feet. Even though these new figures represent a significant change in the PMF, it must be recognized that a storm of this magnitude would devastate the town of Bozeman even without the failure of the dam; and that the dam could be overtopped and breached by a much smaller and more realistic storm with a peak discharge greater than the spillway capacity (780 cfs).

Geologic Stability

Three factors controlling the geologic stability of the dam are seismic hazards, the condition of the foundation, and mass movement near the dam site.

Though only a small percentage of the dam failures in the United States have been caused by earthquakes; the

problem must be addressed, especially in a seismically active area. The U.S. Coast and Geodetic Survey delineated four levels of potential earthquake damage in the United States based on past seismic activity (Fig. 4). Although no seismic frequency is shown on the map, major earthquakes would occur more often in the western U.S. than in the same risk zones in the rest of the country (Algermissen and Perkins, 1976). Mystic Lake dam is located in a zone susceptible to major earthquake damage and has experienced several major shocks in its lifetime, the largest being the Hebgen Lake earthquake of 1959. The bedrock acceleration at Mystic Lake dam, during this event, was estimated to be greater than 0.2g (CH2M Hill, 1980).

The potential for damage from an earthquake depends on both the size of the shock and the proximity of the epicenter to the dam site. The principal hazards to an earth dam from seismic activity include: faulting of the foundation, sliding of the dam embankment due to an increase in pore-water pressure (liquefaction), piping failures through cracks induced by ground motion, a decrease in freeboard on the dam by settlement or tectonic movement, and overtopping of the dam due to seiches produced by ground motion or landslides entering the reservoir (Sherard and others, 1963;

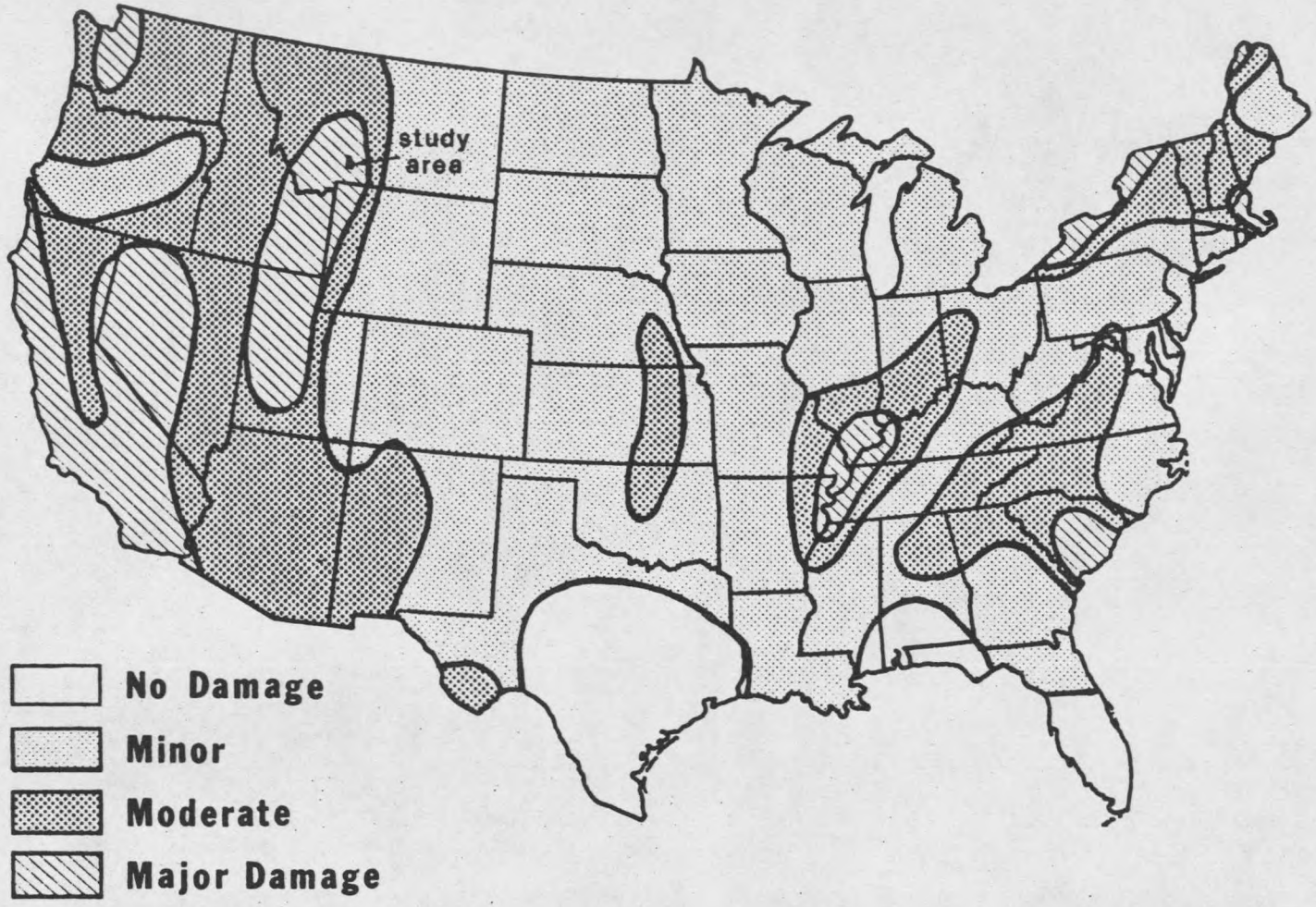

Figure 4. Seismic risk map of the United States showing the potential for damage from earthquake activity. (After Algermissen and Perkins, 1976).

Housner, 1977).

The fact that Mystic Lake dam has survived previous seismic events should not lead to complacency regarding its ability to withstand another major earthquake. The cumulative effects from previous earthquakes are unknown as are the magnitude, location and timing of the next earthquake. It has been estimated that this area could experience a seismic event with a maximum Modified Mercalli intensity of X, (7.3 on the Richter scale), in the next 100 years, and a horizontal acceleration of 0.4g has a 10 percent chance of being exceeded in 50 years (Algermissen and Perkins, 1976; CH2M Hill, 1980).

Two problems mentioned previously in the engineering and construction section are worth repeating in the context of seismic hazards. Seepage water ponding at the toe of the dam (Fig. 2-C) creates a potentially hazardous situation. During an earthquake, high pore-water pressure develops when saturated material is subjected to severe shocks. The resulting liquefaction greatly reduces the shear strength of the embankment or foundation material and causes it to behave as a fluid (Seed, 1973; Wilson and Marsal, 1979). The other problem, differential settlement, is intensified by the ground motion induced by earthquakes. Sherard

(1973, p. 343) reported:

> For a dam that is undergoing relatively large but slow differential settlement, even moderate earthquake shaking could be sufficient to cause abrupt opening of cracks. A combination of moderate differential settlement and a moderate earthquake could result in large cracks.

This implies that differential settlement of Mystic Lake dam may not only be caused by earthquake activity, but may amplify the potential hazards in the event of an earthquake.

The most important consideration in the stability of a dam site is the geologic stability of the foundation (ASCE, 1975). During a drilling program performed by Northern Testing Laboratories in 1977, two drill holes and four probe holes were bored into the foundation of the dam. Standard penetration resistance tests were conducted, samples of the embankment and foundation material were cored, and permeability and pump tests were performed. These tests reveal that the upper dolomite unit of the Amsden Formation, which makes up 15 percent of the west abutment, is fractured and deeply weathered. The Quadrant Quartzite, which underlies the remainder of the west abutment, was reported by Northern Testing Laboratories (1977, p. 2) to be:

> partially to completely decomposed to a medium-grained quartzose sand at the contact, becoming somewhat more massive with depth. The decomposed and fractured areas are very permeable as

> evidenced by pump tests conducted in the foundation bedrock.

The remaining 50 to 60 percent of the dam's foundation and the entire east abutment is located in the landslide debris. Seepage near the east abutment attests to the permeability of the slide debris. The dam's foundation is not anchored in solid, impermeable bedrock; the materials present at the dam site are all fractured, weathered, and exhibit high permeability. According to ASCE (1975, p. 88):

> leakage in the foundation and embankment are the most frequent cause of failures and accidents, even to modern dams.

Since over half the dam is founded in a recent landslide, it is imperative to examine the dam site for evidence of recent mass movement. The landslide at the east abutment of the dam appears to be relatively stable. Trees growing in the deposit are straight and show no signs of recent movement. However, in the toe of the landslide downstream from the dam and in the body of the landslide east of the dam, are numerous indications of recent, small scale mass movement. Rotated blocks with trees leaning uphill along slump scarps are visible as well as "pistol-butted" trees caused by surface creep in the slide deposit. All of these features present on a small scale, indicate that the slide is not in full equilibrium. The slump scarps below the dam

range in height from 2 to 25 feet and are depicted in figure 5. Tree coring to determine the age of the trees with respect to the scarp movement was inconclusive. However, several of the vegetated scarps follow the trend of the roadway and would appear to be related to road construction. If this is true, these scarps are younger than the dam. The lack of vegetation on scarps A and B (Fig. 5) in turn suggests that they are younger than the vegetated scarps. The fact that scarps A and B parallel the dam and are situated below the seepage water pond (Fig. 5) implies that increased pore-water pressure in the slide material may have triggered the latest mass movement. The presence of these scarps directly below the dam raises serious questions as to the stability and safety of the dam.

Downstream Flood Hazards

With the number of housing developments increasing on the floodplain of Bozeman Creek, the potential for damage from the failure of Mystic Lake dam is also increasing. Presently there are 50 residential dwellings and 2 businesses on the east side of town that are affected by the 100-year frequency flood, (one percent chance of occuring in a given year) (U.S. Soil Conservation Service, 1980).

In a letter to the Corps of Engineers, included in

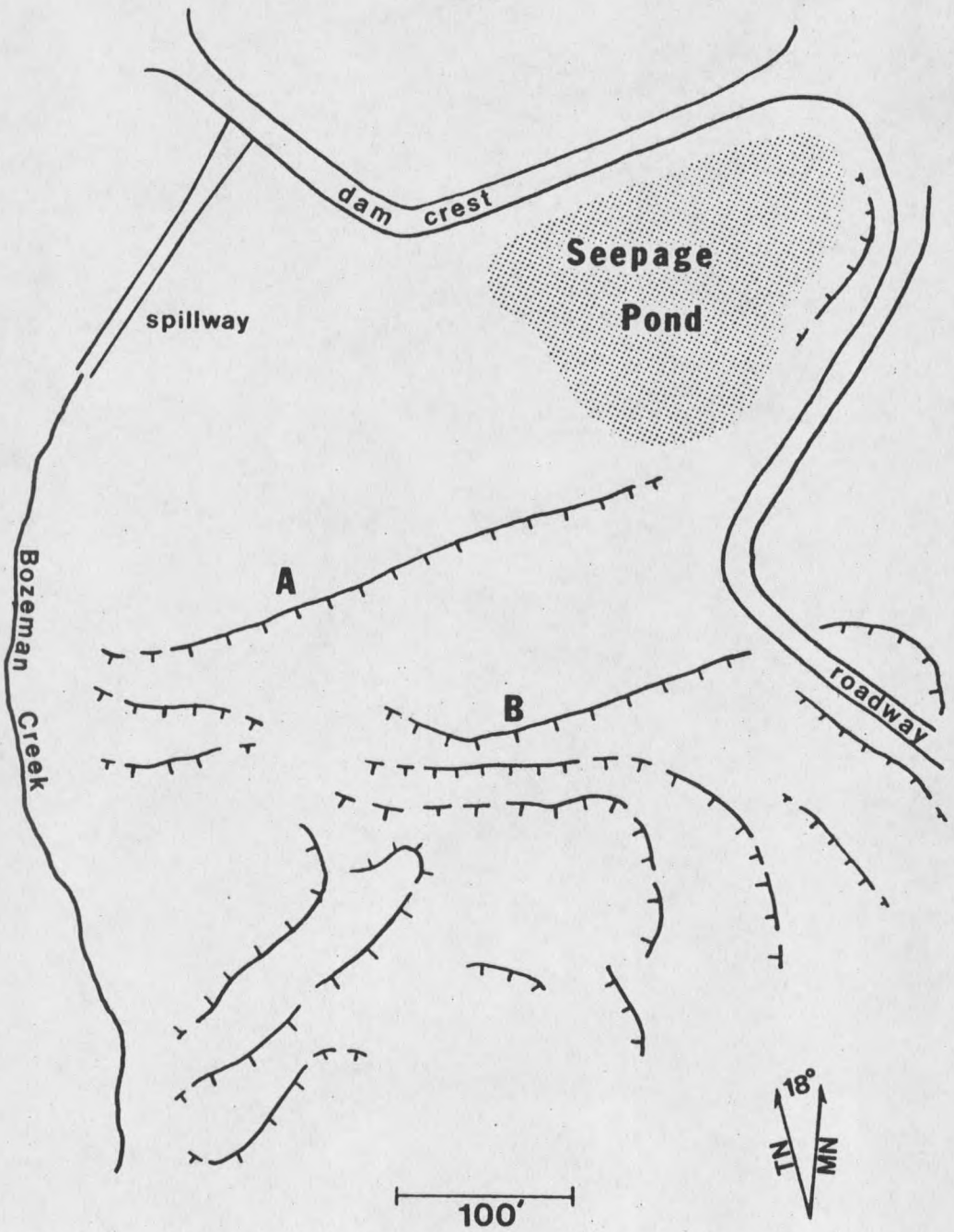

Figure 5. Location map of slump scarps in the toe of the landslide below the dam. Scarps A and B are unvegetated, all others are vegetated. Hachures denote downthrown blocks. Slump scarps are attributed to increased pore-pressure from the seepage water pond.

appendix 4 of the CH2M Hill report (1980), Bozeman City Engineer, Art Van't Hul proposed that the failure of the dam would not cause extensive property damage or loss of life because:

> the area immediately downstream of the mouth of the canyon opens up onto flat alluvial fans that would spread any waters over a fairly wide area.

Several canyons along the Gallatin Range front have alluvial fans, but Bozeman Creek is not one of them. The stream system has entrenched itself into what may have been an alluvial fan, but is presently unrecognizable as such. From the mouth of the canyon, Bozeman Creek is incised into a narrow floodplain that would restrict the flow of water rather than allow it to spread out as Van't Hul has proposed.

There are 17 bridges and culverts that convey the flow of water where roads or bridges are constructed across Bozeman Creek. Of the 17, only 4 do not flow at capacity during the 100-year event, 9 flow at capacity and 4 are overtopped by the same frequency flood (U.S. Soil Conservation Service, 1972). These estimates were made assuming that the flow through the culverts would not be blocked by ice or other debris. Any restrictions at the bridges or culverts could cause major flood damage to the areas upstream from these constrictions (U.S. Soil Conservation Service, 1972).

Several major east-west roads south of town have been constructed above the elevation of the floodplain. Since the culverts and bridges at these crossings are not designed to handle large flood events, water will back up, flooding the area upstream until the roadway is overtopped.

A combination of the housing developments south of town, the lack of an alluvial fan at the canyon mouth, and the number of low capacity bridges and culverts conveying the flow of water in Bozeman Creek, would create a potentially hazardous situation if the dam failed.

A significant body of evidence points to the instability of Mystic Lake dam and to the severe potential of property damage and loss of life in the event of the dam's failure. The remainder of this paper is devoted to describing a model to predict the extent of flooding from the failure of the dam.

MODEL DESCRIPTION

Introduction

The implementation of a model to simulate the failure of the dam and the movement of the floodwave requires measurements or estimates (when measurements are not possible) of the behavior of the real system. The real system can never be measured completely, and for that reason a model, no matter how detailed, can never fully simulate the real system (Zeigler, 1976). A balance must be reached between the cost of data collection, model implementation, and the desired accuracy of the model. The combination of the best available model and a realistic set of data requirements, insures the best possible approximation of the real system.

Models can be broken into three basic groups: physical, symbolic, and analog. A physical model is a representation of the real system by a look-alike model that shares dynamically similar characteristics with the natural system (usually with a reduction in scale). A symbolic model approximates the real system by a "mathematical description of an idealized situation that shares some structural properties of the real system" (Miller and Woolhiser, 1975, p. 367). An analog model is a hybrid between a physical and a symbolic model. The real system is depicted by a network of electronic circuits arranged in accordance to equations from

electronic theory, analogous to the equations from a symbolic model (Chow, 1964).

Since all three types of models have both merits and drawbacks, what constitutes "the best available model" depends heavily on the availability of equipment, previous experience of the modeller, and the cost of implementation in time and money. A symbolic model is considered the best choice for this study based on the following reasons: the availability of a digital computer; previous experience with FORTRAN programming; the lack of experience and equipment to generate an analog model; and the forseen difficulties in reproducing an accurate scale physical model.

The description of the model is broken into two components. The first simulates the development of a time-dependent breach and the resulting outflow hydrograph. The second component simulates the movement of the floodwave through the channel downstream from the dam.

Dam Failure

This portion of the model is also subdivided into two sections. The first deals with the development of the breach and the second approximates the outflow hydrograph through the breach.

Breach development. A breach is the opening created by the failure of a dam through which impounded water escapes. There are two major types of breaches--surface and deep (Yevjevich, 1975). A surface breach is an opening eroded into the crest of the dam that allows free-surface flow to take place, (the free-surface being the air-water interface) (Chow, 1964). A deep breach involves flow under pressure through an opening below the surface of the reservoir. The type of breach is generally determined by the mode of failure. Surface breaches are associated with overtopping of the dam by rain storms, seismically induced settlement or seiches. Deep breaches are caused by piping of the embankment material or failure of the outlet works (Yevjevich, 1975). Because of the complex nature of deep breaches, only a surface breach is simulated in this study. The hypothetical failure is induced by overtopping of the dam by a rain storm producing a discharge into the lake greater than the spillway capacity (780 cfs). The reservoir is assumed to be at capacity at the time of failure. Since it is impossible to accurately predict the shape of the breach it is assumed to take on a triangular form with side slope of 1 to 1.

Even though most breaches develop by progressive erosion (Yevjevich, 1975; Fread, 1978), the majority of

modellers have assumed the breach to be instantaneous and complete (encompassing the entire dam), (Stoker, 1948; 1957; Dressler, 1954; U.S. Army Corps of Engineers, 1957; 1960; 1961; Vasiliev, 1970; Thomas, 1972; Sakkas and Strelkoff, 1973; Yevjevich, 1975; Glass and others, 1976; Gundlach and Thomas, 1977; Rajar, 1978; U.S. Soil Conservation Service, 1979). The assumption of a complete and instantaneous breach, while being attractive for mathematical simplicity, is not realistic for the simulation of most dam failures. This is especially true in the case of earth-fill dams which require a finite amount of time for the breach to attain its final size (Fread, 1978). Other investigators (Balloffet and others, 1974; Fread, 1978; 1980; Fread and Harbaugh, 1973), while recognizing the importance of time in the development of the breach, assumed a constant rate of erosion.

In this model the rate of breach erosion is assumed to increase exponentially as a function of time. Figure 6 illustrates the development of a time-dependent, triangular surface breach. The area of the breach at any time step, may be expressed as:

$$\text{Area} = \text{Breach Depth}^2 \qquad (1)$$

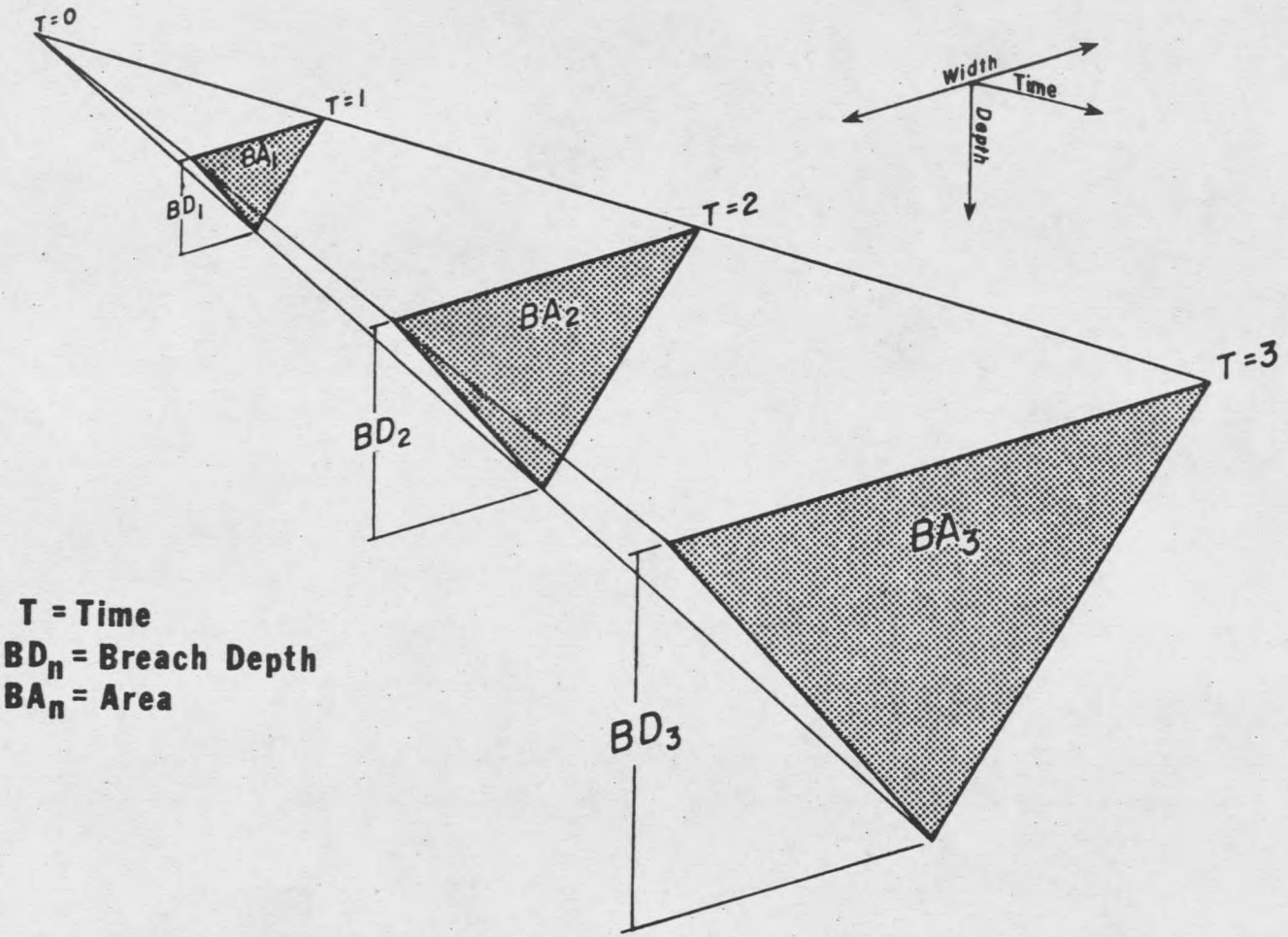

Figure 6. Erosional development of a triangular surface breach through time. The breach depth (BD) increases linearly with time while the breach area (BA) increases exponentially as a function of depth, ($BA = BD^2$).

The breach area, therefore, increases exponentially as a function of depth. The breach depth, on the other hand, increases linearly as a function of time:

$$\text{Breach Depth} = \text{Time} \times \text{Dam Height}/\text{Failure Time} \quad (2)$$

where the ratio of Dam Height/Failure Time establishes the rate of change of the breach depth in feet/sec. The maximum dimensions of the breach are governed by the dam height or the depth to bedrock. It is assumed that once the base of the breach has reached bedrock downcutting will cease. Lateral erosion would continue until the flow velocity in the breach decreased. However, for simplicity, this factor is ignored. The failure time for Mystic Lake dam, used in equation 2, is estimated to be in the range of 5 to 10 minutes, based on the following evidence. Buffalo Creek dam, an earth-fill structure of comparable size, was overtopped by a rain induced flood and failed in approximately 5 minutes (Fread, 1978). Also according to Foster (CH2M Hill, 1980, p. v), "the dam is constructed of materials that would quickly erode and fail when overtopped by flood-waters." Based on these two lines of evidence the estimated failure time seems reasonable.

Breach hydrograph. The discharge from a breached dam plotted as a function of time is known as a breach hydrograph. In order to show the effects of flooding from the failure of Mystic Lake dam, a breach hydrograph must be generated.

Previous investigators have assumed the flow through a breached dam could be approximated by the equations describing broad-crested weir flow (U.S. Corps of Engineers, 1957; 1960; 1961; Fread, 1978; 1980; Fread and Harbaugh, 1973). A major problem with this assumption involves the length of the weir flow channel. The breach channel not only increases in depth through time, but increases in length as well; eventually attaining a length greater than 200 feet. According to Tracy (1957, p. 2):

> for very small head-to-length ratios, the weir crest becomes a reach of open channel in which frictional resistance predominates, and for which the discharge is more properly evaluated by one of the open channel flow formulas than by a weir formula.

The flow through a breached dam is classified as gradually to rapidly-varied, unsteady flow because the velocity varies with time and space. However, for simplicity, unsteady flow can be treated as steady flow if the change in the flow conditions over the time step is negligible (Chow,

1959). Manning's equation for steady flow, used in this model to approximate the outflow from the breach, is written as:

$$Q = \frac{1.49}{n} A R^{2/3} S^{1/2} \qquad (3)$$

where Q is the discharge, A is the cross-sectional area, R is the hydraulic radius, S is the channel slope, and n is the Manning's roughness coefficient.

Using Manning's equation, the discharge is calculated as a function of the effective area of flow in the breach. As the breach area increases, the discharge of water escaping through the breach increases as well, causing the lake level in the reservoir to decrease. Figure 7 illustrates the development of the breach area (BD^2) and the drop in the lake level (ΔL) as a function of time. The difference between the elevation of the lake level and the base of the breach, at a given point in time (Fig. 7), defines the depth of flow (FD) and the effective area of flow (FD^2).

The lake level at any point in time (Fig. 7) is a function of the discharge during the previous time step. By expressing the lake level as a function of the reservoir volume (Fig. 8) the lake level can be determined as a function of the discharge. The discharge, in turn, is a function of

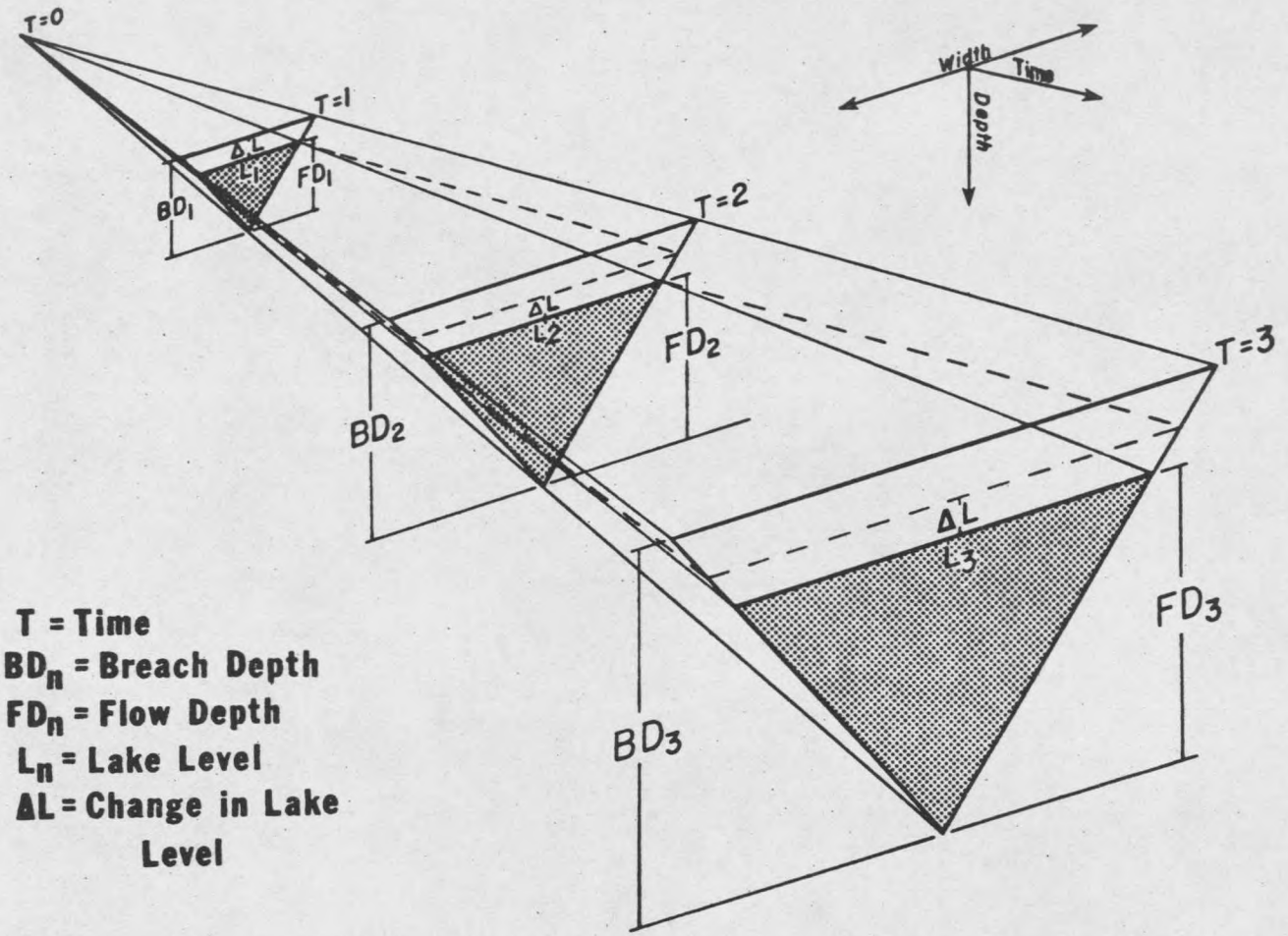

Figure 7. As the breach area increases with time, the discharge through the breach increases causing a drop in the lake level (ΔL). The depth of flow (FD) and the effective area of flow (FD^2) at any time step is defined by the lake level (L) and the breach depth (BD).

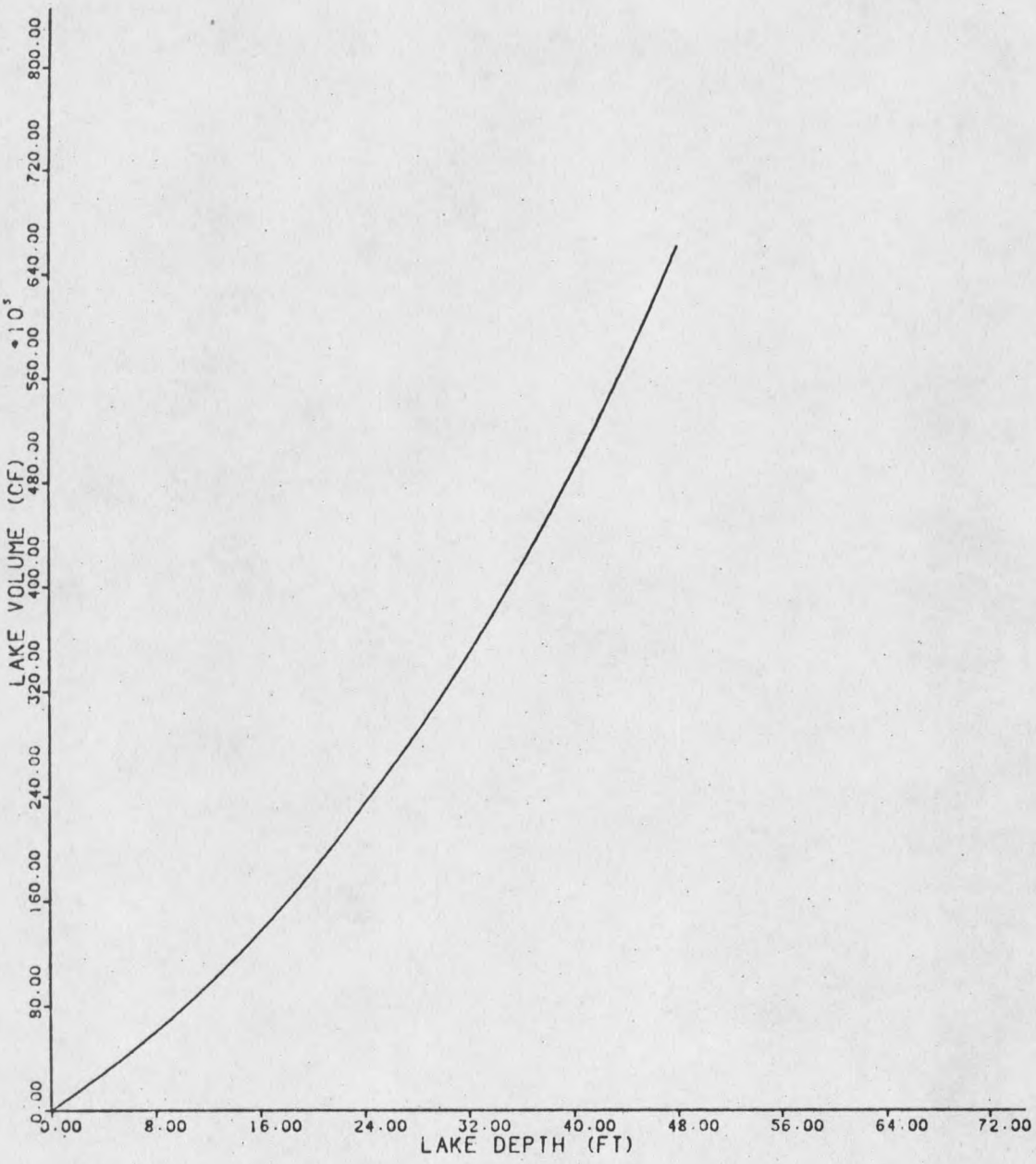

RESERVOIR DEPTH-VOLUME CURVE

Figure 8. Curve defining the volume of Mystic Lake as a function of the reservoir depth. (From CH2M Hill, 1980).

the effective area of flow defined by the lake level and the breach area. The relationship between the discharge and the lake level is such that the lake level must be known in order to calculate the discharge.

A "known" value for the lake level can be approximated by projecting the change in the lake level (ΔL), (Fig. 7) from the previous time step to calculate the lake level at the present time step:

$$\Delta L = \text{Lake Level}_{i-2} - \text{Lake Level}_{i-1} \quad i=2,3...n \tag{4}$$

$$\text{Lake Level}_{i} = \text{Lake Level}_{i-1} - \Delta L \tag{5}$$

For example in figure 7, the lake level L_3 can be projected by subtracting (ΔL), the difference between the lake levels L_1 and L_2, from the lake level L_3. The "known" lake level is then used to calculate the effective area of flow and the corresponding instantaneous discharge from the breach.

The total discharge from the dam is the sum of the flows contributed by the spillway, outlet gates and the breach. The depth-discharge curves for the spillway and the outlet gates are illustrated in figure 9. By averaging the the discharge calculated at the present time step with the discharge from the previous time step, the volume of outflow over the time step can be computed. The resulting decrease

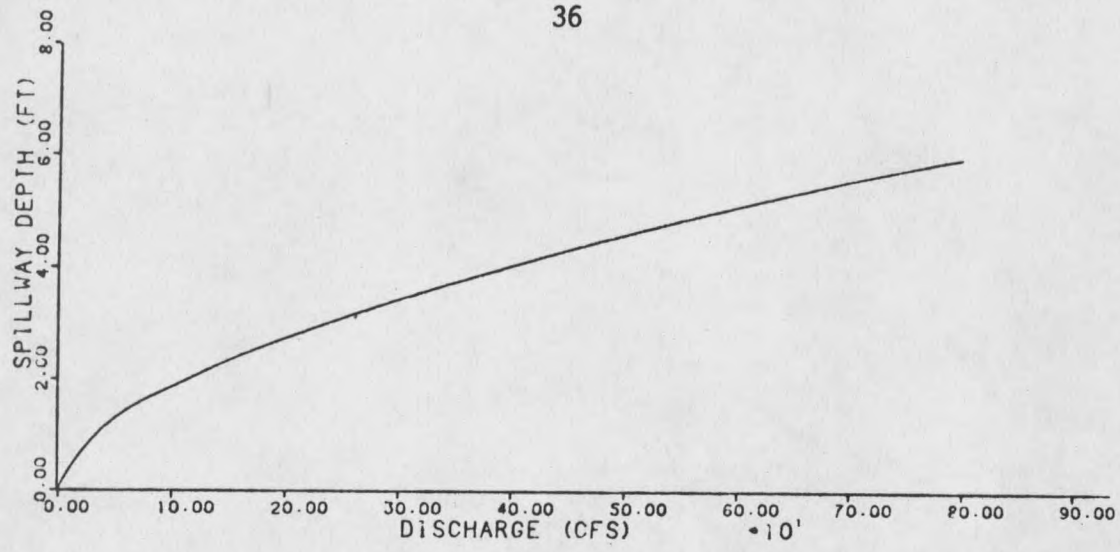

SPILLWAY RATING CURVE

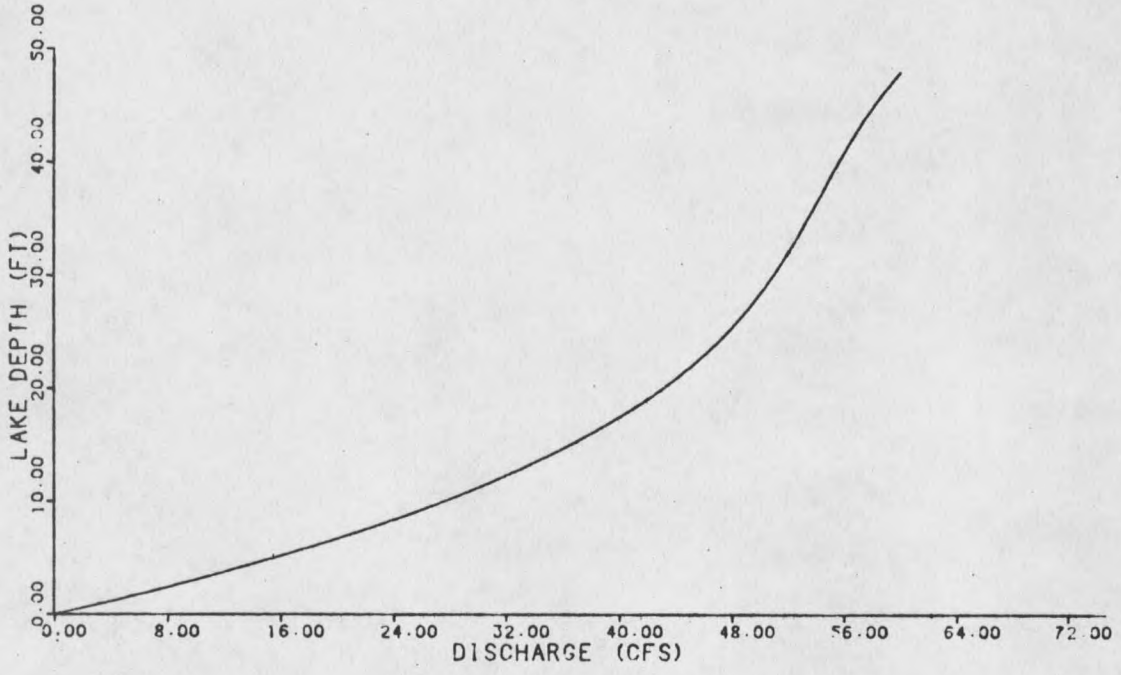

12 & 16" OUTLET PIPES RATING CURVE

Figure 9. Rating curves of discharge as a function of depth for the spillway and outlet gates. (After CH2M Hill, 1980).

in the lake level can be read from the depth-volume curve (Fig. 8). An iterative scheme is used to test the lake level computed from the depth-volume curve (Fig. 8) against the projected lake level from equation 5. If the difference between the projected and calculated lake levels does not fall within a tolerance limit of 0.01 foot, a new ΔL is tested until the difference is negligible.

A hypothetical outflow hydrograph (Fig. 10) is generated for Mystic Lake dam using the following assumptions and initial conditions: a failure time of 7.5 minutes, a time step of 5 seconds, a Manning's n for the breach channel estimated to be .047, the initial lake level at the dam crest, and the inflow into the lake equal to 1000 cfs. The peak discharge, 83,500 cfs, agrees closely with results obtained from an equation developed by Kirkpatrick (1977) for computing the maximum discharge through a breached dam. He arrived at this equation by plotting dam height versus peak discharge from actual dam failures. The equation for the straight line through the points:

$$Q_{max} = 65 \times \text{Dam Height}^{1.85} \qquad (6)$$

yields an estimated peak discharge of 83,800 cfs for Mystic Lake dam, with a crest height of 48 feet.

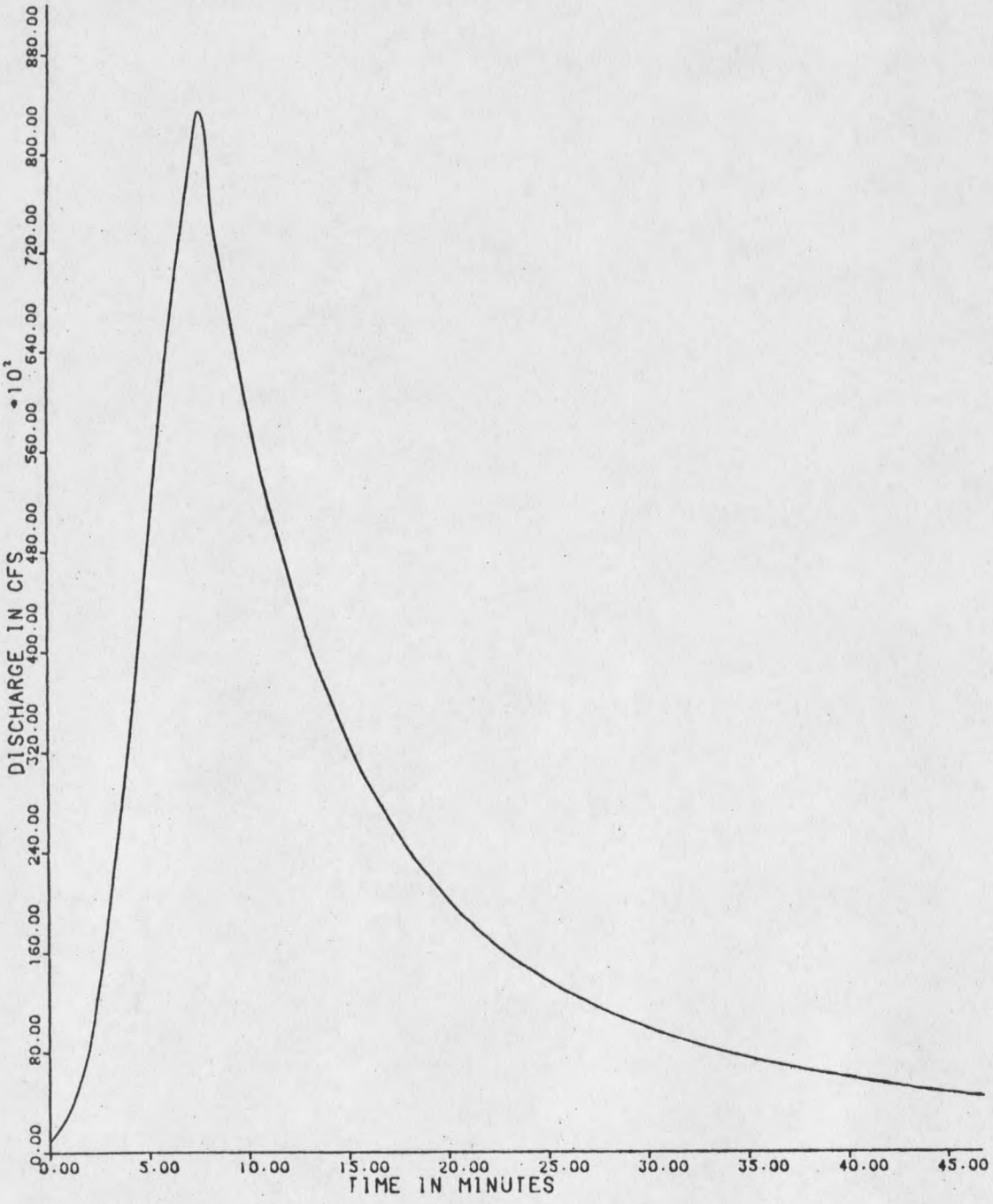

Figure 10. Breach outflow hydrograph from the hypothetical overtopping of Mystic Lake dam. The peak discharge from the failure, 83,500 cfs, is reached in 7.5 minutes.

Downstream Routing

Introduction. Having developed a time-dependent surface breach and an outflow hydrograph for Mystic Lake dam, the remainder of the model description involves routing the floodwave downstream. According to Chow (1964, sec. 25, p. 35) flood routing is defined as:

> the procedure whereby the time and magnitude of a flood wave at a point on a stream is determined from the known or assumed data at one or more points upstream.

The enumeration and comparison of all flood routing methods is beyond the scope and purpose of this study. For this reason, routing methods will be discussed and compared only in general terms. For an in-depth evaluation, the reader is directed to: Thomas, 1934; Gilcrest, 1950; Chow, 1959; 1964; Yevjevich, 1964; Brakensiek and Comer, 1965; and Miller and Cunge, 1975.

The downstream routing section of the model description is divided into two portions. First, the criteria for choosing a flood routing method are discussed, followed by a description of the numerical techniques used to solve the routing equations.

Selection of a routing method. Flood routing methods fall into two basic categories--hydraulic and hydrologic. The hydraulic methods are based on the complete equations of unsteady flow derived by de Saint-Venant (1871). These equations arise from the laws of conservation of mass and momentum applied to open channel flow. Matter is a form of energy, and as such, conforms to the laws of conservation. The continuity equation for the conservation of mass is expressed as:

$$\frac{\partial Q}{\partial x} + \frac{\partial A}{\partial t} - q = 0 \qquad (7)$$

where Q is the discharge, A is the cross-sectional area, x is the distance, t is the time, and q is the lateral inflow or outflow per unit stream length (inflow is positive and outflow is negative). Equation 7 states that as the discharge varies with distance at a rate $\partial Q/\partial x$, the cross-sectional area of flow must change with time at a rate $\partial A/\partial t$. Since water is incompressible, the net change in the discharge plus the change in the area is zero, and the total mass of the system remains unchanged (Chow, 1959).

It is convenient to re-write equation 7 so that the change in area $\partial A/\partial t$ can be expressed as a function of depth (Amein and Fang, 1970). Equation 7 then becomes:

$$\frac{\partial Q}{\partial x} + B\frac{\partial y}{\partial t} - q = 0 \qquad (8)$$

where y is the depth and B is the top width of the stream, defined as the derivative dA/dy.

Not only must the mass of the system be conserved but the momentum as well. The momentum equation accounts for the change in the energy of the system due to the the effects of friction and acceleration, and is expressed as:

$$\frac{\partial Q}{\partial t} + \frac{\partial Q^2/A}{\partial x} + gA\left(\frac{\partial y}{\partial x} + S_o + S_f\right) = 0 \qquad (9)$$

where g is the gravitational constant, S_o is the channel bottom slope, and S_f is the friction slope evaluated using Manning's equation:

$$S_f = \frac{n^2\, Q^2}{2.2\, A^2\, R^{4/3}} \qquad (10)$$

The derivation of equations 7-9 is found in the following references: de Saint-Venant, 1871; Gilcrest, 1950; Chow, 1959; Amein and Fang, 1970; Liggett, 1975.

While the hydraulic methods are based on the complete equations of unsteady flow, the hydrologic methods present a more simplified approach to the problem. Only the continuity equation is utilized to approximate the behavior of the real system. The effects of acceleration and frictional

resistance accounted for in the momentum equation are ignored (Miller and Cunge, 1975).

The choice between the two routing methods should be governed by the following considerations: the accuracy of the equations in reproducing the behavior of the real system, the ease of computations in arriving at a solution, and the amount of computer time required to perform the simulation. Because the hydrologic method uses only the continuity equation, it can be applicable only in situations where the effects of acceleration and frictional resistance are negligible (Fread, 1980). The rapidly-varied unsteady flow associated with dam-break floodwaves has appreciable acceleration effects and cannot be described by any hydrologic method (Miller and Cunge, 1975). The only way to successfully model these flow conditions is with a hydraulic method utilizing the complete equations of unsteady flow. The hydraulic methods yield a more accurate representation of the real system, but at the cost of rigorous computations and increased computer time. Equations 8-9 constitute a system of non-linear hyperbolic partial differential equations. The independent variables contained in the equations are x and t, the dependent variables are y and Q; the remaining terms are either constants or functions of x, t, y

and/or Q. This system of equations cannot be solved by analytical methods; the only alternative for solution is the utilization of numerical techniques (Amein and Fang, 1970; Fread, 1980).

Numerical solution. There are a large number of numerical methods, but only two are applicable to hyperbolic partial differential equations; the method of characteristics and finite difference methods (Liggett and Cunge, 1975). Because of the complexity of the characteristic method, only finite difference methods will be analyzed and compared. Further information concerning numerical methods and their applications to flood routing may be found in the following references: Richtmyer, 1962; Brakensiek, 1966; Amein, 1967; Liggett and Woolhiser, 1967; Strelkoff, 1970; Vasiliev, 1970; Abbott, 1975; Liggett and Cunge, 1975; Vasiliev and others, 1976.

Of the available finite difference schemes, the two most commonly used in numerical flood routing are the explicit and implicit methods. The decision to employ an implicit method was based on the conclusions of previous investigators (Abbott and Ionescu, 1967; Ameir, 1967; 1968; Liggett and Woolhiser, 1967; Amein and Fang, 1969; 1970; Chaudhry and Contractor, 1973; Price, 1974; Amein and Chu,

1975; Greco and Panattoni, 1975; Liggett and Cunge, 1975; Miller and Cunge, 1975; Fread, 1978; 1980; Ponce and others, 1978). According to their findings, the implicit methods, although more difficult to use, are very flexible and can handle unequal time and distance steps. The implicit methods are also unconditionally stable and are not restricted to very small time steps like those required for the explicit schemes. Stability here refers to the introduction of errors into the solution procedures. A large time step used in a conditionally stable scheme, like the explicit method, causes small errors to grow exponentially until the computation "blows-up". The implicit method, being unconditionally stable, allows for the selection of a time step governed only by convergence. The concept of convergence implies that as Δx and Δt approach zero, the computation tends towards an exact solution (Fread, 1974a; Liggett and Cunge, 1975). However, as Δx and Δt become smaller, the roundoff error increases (D., Dyreson, oral commun., 1981).

Of the various implicit schemes available for use, the weighted four-point method developed by Preissmann (1961) and used by Amein and Fang (1970), Chaudhry and Contractor (1973), Greco and Panattoni (1975) and Fread (1978; 1980) is considered the best implicit method for this study because

of its ability to model streams with variable cross-sections and bed slope.

The four-point implicit scheme numerically solves equations 8-9 by replacing the partial derivatives with a corresponding set of finite difference algebraic expressions. The solution of the algebraic expressions are sought over a discrete time-distance grid illustrated in figure 11. Time lines are drawn parallel to the distance-axis, with spacing Δt, which need not be constant, and are designated by the superscript j. The distance lines, parallel to the time-axis, represent the locations of cross-sections along the stream with spacing Δx, which also need not be constant. The subscript i identifies the spatial location. Location i=1 is the upstream boundary and i=N is the downstream boundary. The grid points or nodes at the intersections of the time-distance lines represent the points in time and space where the solutions for depth and discharge are sought.

Derivatives in the weighted four-point implicit scheme are represented by the following algebraic expressions where K represents any variable. The time derivatives are approximated using a forward difference quotient centered between nodes i and i+1 along the distance axis:

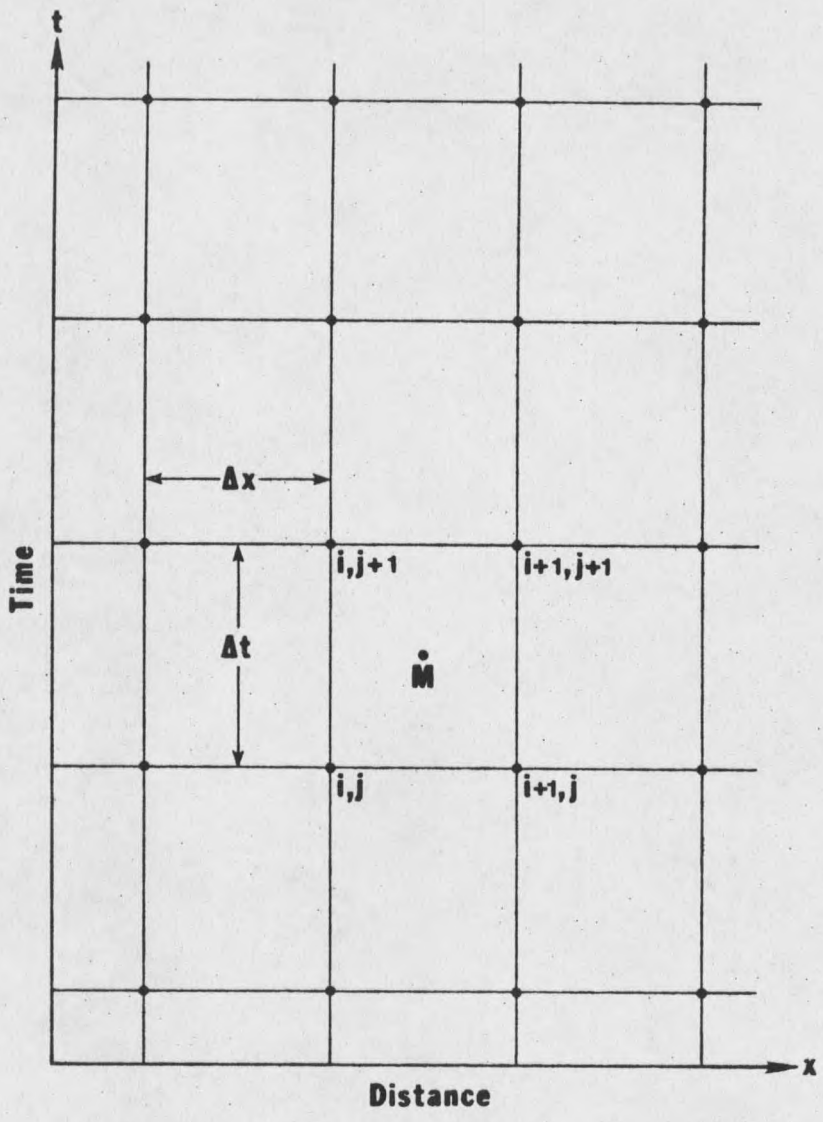

Figure 11. Discrete time-distance grid for the solution of the four-point implicit method. Time lines are designated by j and distance lines by i. The solution of the continuity and momentum equations is sought at point M.

$$\frac{\partial K}{\partial t} = \frac{K_i^{j+1} + K_{i+1}^{j+1} - K_i^j - K_{i+1}^j}{2\Delta t} \qquad (11)$$

The spatial derivatives are also approximated by a forward difference quotient, but its position between two adjacent time lines, j and j+1, is controlled by the weighting factors θ and $1-\theta$:

$$\frac{\partial K}{\partial x} = \theta \left(\frac{K_{i+1}^{j+1} - K_i^{j+1}}{\Delta x} \right) + (1-\theta) \left(\frac{K_{i+1}^j - K_i^j}{\Delta x} \right) \qquad (12)$$

weights the influence of the values on the two adjacent time lines. When θ is 1.0 only the values on the j+1 time line influence the solution and a fully implicit or backward difference scheme results (Fread, 1978). A weighting factor of 0.5 yields the box scheme proposed by Amein and Fang (1970) which equally weights the values on both time lines. The influence of the weighting factor θ on the accuracy of the computations was examined by Chaudhry and Contractor (1973), Fread (1974a) and Ponce and others (1978). They concluded that the accuracy drops off as θ departs from 0.5 and approaches 1.0. A value of 0.6 for θ minimizes the loss of accuracy (Fread, 1974a; 1978), and reduces the pseudo instability reported by Chaudhry and Contractor, (1973).

Variables other than derivatives are evaluated at the same location in time and space as the derivatives by:

$$K = \Theta \left(\frac{K_i^{j+1} + K_{i+1}^{j+1}}{2} \right) + (1-\Theta) \left(\frac{K_i^j + K_{i+1}^j}{2} \right) \qquad (13)$$

When the derivatives and other variables in equations 8 and 9 are replaced by the finite difference operators from equations 11 through 13, the following four-point implicit finite difference equations are obtained:

$$\Theta \left(\frac{Q_{i+1}^{j+1} - Q_i^{j+1}}{\Delta x} \right) + (1-\Theta) \left(\frac{Q_{i+1}^j - Q_i^j}{\Delta x} \right) + \left\{ \Theta \left(\frac{B_i^{j+1} + B_{i+1}^{j+1}}{2} \right) + (1-\Theta) \left(\frac{B_i^j + B_{i+1}^j}{2} \right) \right\} \left(\frac{y_i^{j+1} + y_{i+1}^{j+1} - y_i^j - y_{i+1}^{j+1}}{2\Delta t} \right) - q = 0 \qquad (14)$$

$$\left(\frac{Q_i^{j+1} - Q_{i+1}^{j+1} - Q_i^j - Q_{i+1}^j}{2\Delta t} \right) + \Theta \left(\frac{(Q^2/A)_{i+1}^{j+1} - (Q^2/A)_i^{j+1}}{\Delta x} \right) + (1-\Theta) \left(\frac{(Q^2/A)_{i+1}^j - (Q^2/A)_i^j}{\Delta x} \right) + g \left\{ \Theta \left(\frac{A_i^{j+1} + A_{i+1}^{j+1}}{2} \right) + (1-\Theta) \left(\frac{A_i^j + A_{i+1}^j}{2} \right) \right\} \left\{ \Theta \left(\frac{y_{i+1}^{j+1} - y_i^{j+1}}{\Delta x} \right) + (1-\Theta) \left(\frac{y_{i+1}^j - y_i^j}{\Delta x} \right) + \right.$$

$$S_0 + \theta \left\{ \left(S_f \, {}^{j+1}_{i+.5}\right) + \left(S_f \, {}^{j}_{i+.5}\right) \right\} = 0 \qquad (15)$$

where all variables with the superscripts j are known, while those with superscripts j+1 are unknown.

Unlike the explicit system where unknown values are extrapolated from a previous time step, the four-point implicit method solves for the unknowns on the next time line by a Newton-Raphson iterative scheme (Amein and Fang, 1969; Fread, 1980). Assuming that all variables at each node along the time line j are known from initial conditions or previous computations, trial values for the unknowns at j+1 are established equal to the known values at j. These "implied" values are tested by evaluating the continuity and momentum equations, 14 and 15, at point M in each of the t-x grid blocks. Equations 14 and 15 cannot be solved in a direct manner because there are only two equations and four unknowns. However, any two neighboring grid blocks share two unknowns in common. Since there are N nodes or cross-sections along the distance-axis, there are N-1 grid blocks with N-1 interior points M. By applying equations 14 and 15 simultaneously to point M in each grid block, a total of 2N-2 equations for the solution of 2N unknowns result. Two

additional equations describing the depth-discharge relationships at the upstream and downstream boundaries complete the system of 2N simultaneous equations. When the stream flow is supercritical, flow disturbances cannot travel upstream; therefore the downstream boundary becomes superfluous. Instead two boundary conditions are required at the upstream boundary (Fread, 1980). If the flow is subcritical, the breach discharge as a function of time satisfies the upstream boundary condition, while an equation for the depth-discharge rating curve fulfills the downstream boundary condition.

The 2N simultaneous equations can be readily solved by representing them in a matrix configuration (Amein and Fang, 1969; 1970; Fread, 1978; 1980). Three matrices A, R and S (Fig. 12) are generated. A is a coefficient matrix composed of partial derivatives of each equation with respect to each unknown in the equation. Matrix R is a vector of residuals from the solution of the continuity and momentum equations at point M in each of the grid blocks. The solution vector S can be obtained by a variety of matrix manipulations such as the Gaussian elimination or matrix inversion (Amein and Fang, 1969). Gaussian elimination is the first method taught in beginning algebra for the solution of simultaneous

$$A = \begin{bmatrix} a_{11} & a_{12} & & & & & & \\ a_{21} & a_{22} & a_{23} & a_{24} & & & & \\ a_{31} & a_{32} & a_{33} & a_{34} & & & & \\ & & a_{43} & a_{44} & a_{45} & a_{46} & & \\ & & a_{53} & a_{54} & a_{55} & a_{56} & & \\ \cdots & \cdots & \cdots & \cdots & \cdots & \cdots & \cdots & \cdots \\ \cdots & \cdots & \cdots & \cdots & \cdots & \cdots & \cdots & \cdots \\ & & & a_{2N-2,2N-3} & a_{2N-2,2N-2} & a_{2N-2,2N-1} & a_{2N-2,2N} & \\ & & & a_{2N-1,2N-3} & a_{2N-1,2N-2} & a_{2N-1,2N-1} & a_{2N-1,2N} & \\ & & & & & a_{2N,2N-1} & a_{2N,2N} & \end{bmatrix} \quad R = \begin{bmatrix} r_1 \\ r_2 \\ r_3 \\ r_4 \\ r_5 \\ \cdots \\ \cdots \\ r_{2N-2} \\ r_{2N-1} \\ r_{2N} \end{bmatrix} \quad S = \begin{bmatrix} s_1 \\ s_2 \\ s_3 \\ s_4 \\ s_5 \\ \cdots \\ \cdots \\ s_{2N-2} \\ s_{2N-1} \\ s_{2N} \end{bmatrix}$$

Figure 12. Matrices A, R and S for the solution of simultaneous equations. The elements of matrix A are the partial derivatives of the continuity and momentum equations with respect to the unknowns Q and y on the time line j+1. Matrix R is a vector of residuals from the solution of the continuity and momentum equations at point M (Fig. 11). The solution vector S cortains the residuals from the trial values of Q and y on the time line j+1.

equations (although most teachers mercifully omit the name). Unknowns are eliminated mathematically until the system is reduced to one equation and one unknown. The remaining unknowns are then calculated by back substitution (James and others, 1977).

The values in the solution vector S are residuals from the trial values of the unknown depths and discharges. S_1, S_3, S_5 . . . and so on, are the depth residuals at cross sections one, two and three respectively. S_2, S_4, S_6 . . . and so on, are the corresponding discharge residuals for the same cross-sections. The range of these values are tested within a tolerance limit of 0.05 foot for depth, and 50.0 cfs for discharge. If any of the values fall outside the specified range, each residual is added or subtracted (depending on its sign) to its corresponding unknown value. These corrected values are then used to generate new matrices A, R and S and the procedure is repeated until the residuals "zero-out". Once the unknowns on the j+1 time line have been solved, they now become the "known" values and the time step is incremented by Δt. With each change in the time step, a new value for the discharge is calculated from the breach hydrograph at the upstream boundary. The whole procedure of establishing trial values, generating

matrices, "zeroing-out" the residuals and incrementing the time step is repeated until the flood has been routed through the channel.

Data requirements. In order to solve the equations of unsteady flow and simulate the movement of the wave downstream, all variables and their inter-relationships must be known or assumed at points along the stream channel.

The first step is to define the geometry of the stream channel with a series of cross-sectional profiles perpendicular to the direction of flow. The profiles are drawn using survey data or, when costs are prohibative, a 1:24,000 scale map with a 20 foot contour interval (Glass and others, 1976; Fread, 1978). In this study, profiles were acquired from both data sources. Cross-sections in the canyon were taken from a 1:24,000 scale map, and those from the canyon mouth through Bozeman were obtained from U.S. Soil Conservation Service survey data (R. Bergantine, personal commun., 1981). The cross-sections were established at points of "inflection" (Fig. 13) to record any changes in the geometry.

The area at each cross-section is plotted as a function of depth (f(y)), (Fig. 14) and is represented by a third order polynomial:

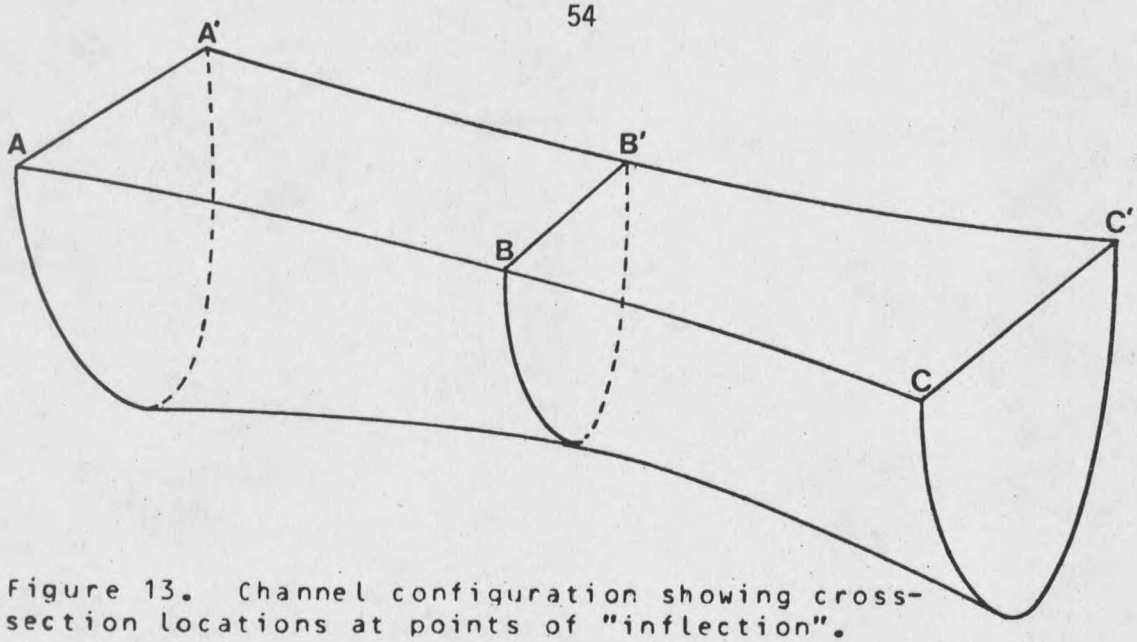

Figure 13. Channel configuration showing cross-section locations at points of "inflection".

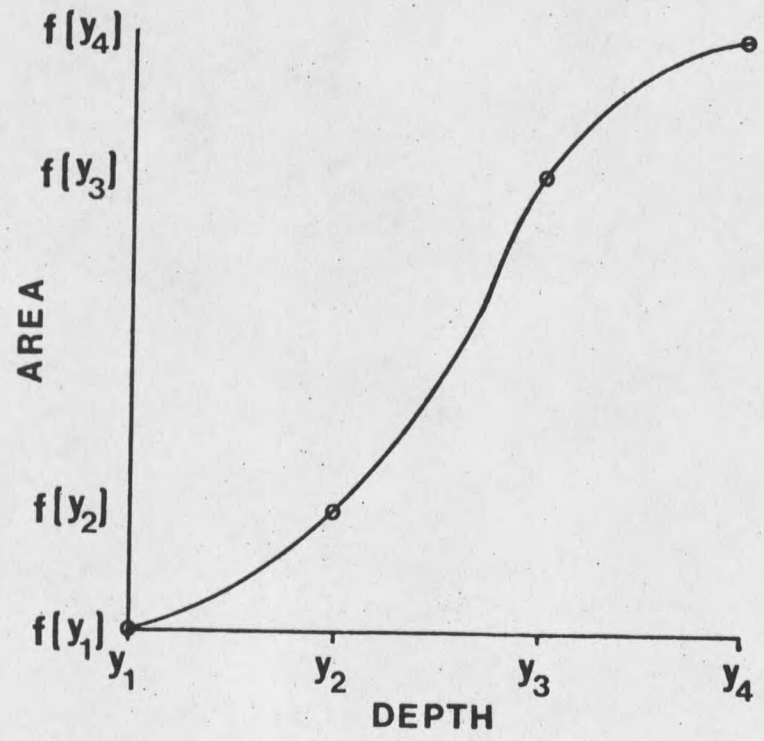

Figure 14. Cross-sectional area f(y) as a function of depth for any cross-section A-A', B-B' or C-C' (Fig. 13).

$$\text{Area} = f(y) = a + by + cy^2 + dy^3 \qquad (16)$$

where y is the depth and a, b, c and d are coefficients. The coefficients are calculated by solving 4 equations, in the form of equation 16, simultaneously in a matrix configuration (Fig. 15). The values in the solution vector S, are the coefficients a, b, c and d, obtained by Gaussian elimination.

Where the stream flow divides around an island (Fig. 16-A, B), the total discharge Q is broken into components Q1 and Q2, and the total area A into A1 and A2 (Chow, 1959; Baltzer and Lai, 1968; Cunge, 1975). The whole being equal to the sum of the parts allows the bifurcated channel to be treated as a single cross-section and represented by a single depth-area curve. Once the cross-section positions have been determined, the total stream length is represented by a series of reaches with length Δx which need not be constant.

The rapidly rising hydrograph associated with the dam's failure (Fig. 10) can cause problems of instability and non-convergence even when an implicit technique is employed (Fread, 1978). However, these computational problems can be overcome by the proper selection of the time and distance

$$Y = \begin{bmatrix} y_1 & (y_1)^2 & (y_1)^3 \\ y_2 & (y_2)^2 & (y_2)^3 \\ y_3 & (y_3)^2 & (y_3)^3 \\ y_4 & (y_4)^2 & (y_4)^3 \end{bmatrix} \qquad A = \begin{bmatrix} f(y_1) \\ f(y_2) \\ f(y_3) \\ f(y_4) \end{bmatrix} \qquad S = \begin{bmatrix} a \\ b \\ c \\ d \end{bmatrix}$$

Figure 15. Matrix configuration for the solution of the depth-area coefficients. The elements of matrices Y and A are the values of depth and area from the depth-area curve in figure 14. The values in the solution vector S are the coefficients for a third order polynomial defining the depth-area curve in figure 14.

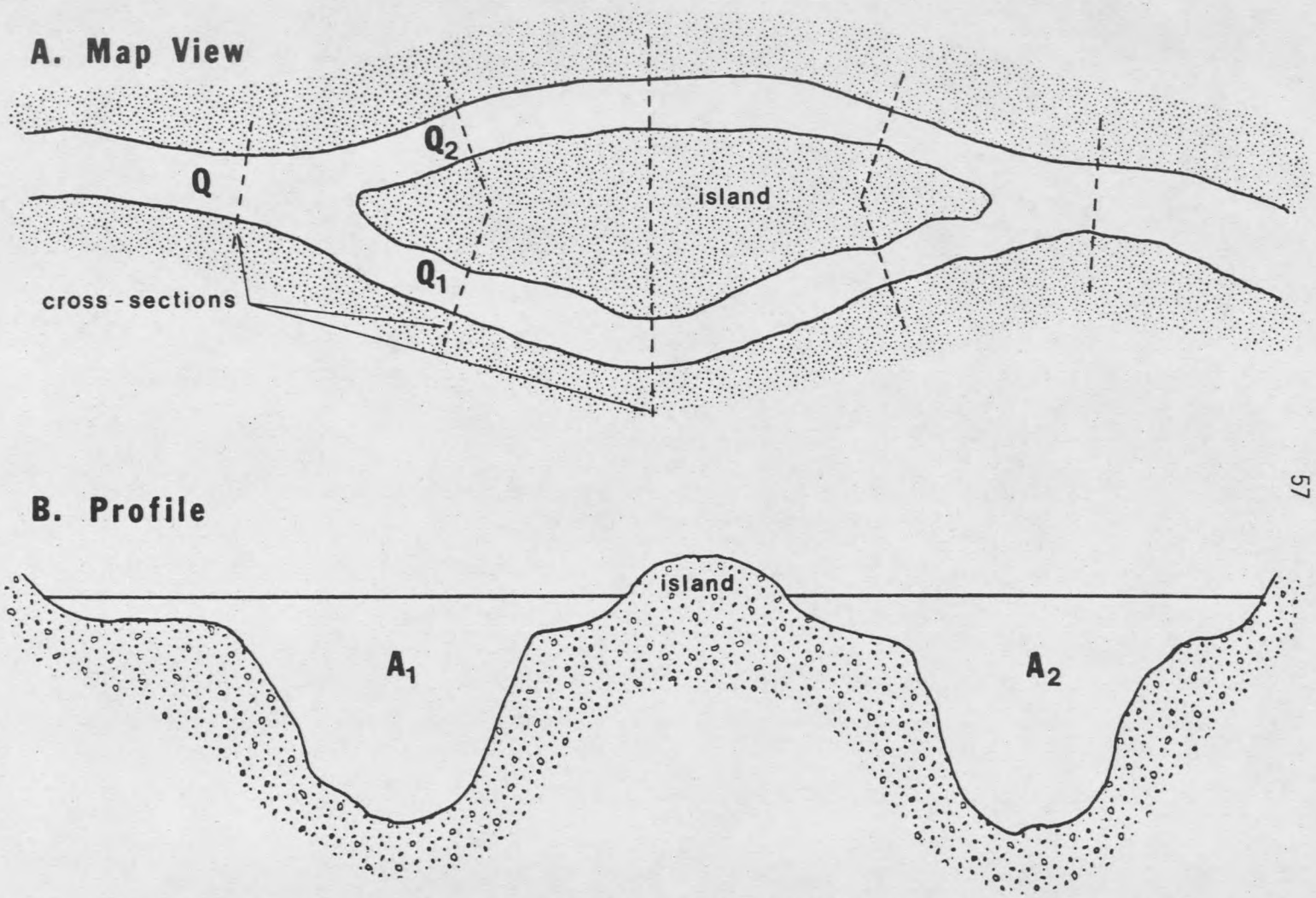

Figure 16. Map and profile view of flow division around an island. The total discharge Q is divided into Q1 and Q2, and the total area A into A1 and A2.

steps. If the time step is too small, or the distance step too large relative to the change in the discharge, negative depths tend to develop in the vicinity of the wave front causing the computation to "blow-up". By increasing the time step and/or decreasing the distance step by inserting additional cross-sections, these problems disappear. However, if the time step is made too large, the procedure fails to converge.

Because the dam-break hydrograph is very peaked, it tends to dampen and flatten out as it moves downstream. This being the case, the time and distance steps are allowed to increase in the downstream direction. Fread (1974a) proposed a guideline for the selection of the time step:

$$\Delta t = \text{Time of Peak Arrival} / 20 \qquad (17)$$

As the floodwave advances, Δt increases because the arrival time of the peak increases at locations further and further downstream. The increase in the time step allows the distance step to increase gradually from 100 feet at the dam to 1200 feet near the downstream boundary.

The initial conditions of depth and discharge at each cross-section must be known at time t=0 in order to solve the unsteady flow equations. The discharge at each cross-

section i is calculated as:

$$Q_i = Q_{i-1} + q_{i-1} \qquad i=2,3,4...n \qquad (18)$$

where Q_1 is the discharge at the dam before the failure from the spillway and outlet gates, and q_1 is the lateral inflow or outflow between sections i and i+1. The lateral inflow contributed by tributaries or overland flow would be significant, however because of a lack of data, it is assumed to be zero. Infiltration losses due to inundation are considered important only when the inundated areas are large and dry before the flood wave arrives (Cunge, 1975). If the dam is overtopped by the discharge from a heavy rainfall, the areas along the stream channel will be saturated and the losses due to infiltration will be negligible (Cunge, 1975).

The depth at each cross-section is calculated by an iterative scheme known as the standard step-backwater method (Chow, 1959; 1964; Bailey and Ray, 1966). Figure 17 illustrates a channel reach of length Δx. Equating the total heads at the end sections 1 and 2 (Fig. 17), the total energy of the system may be written as:

$$Z_1 + V_1^2/2g = Z_2 + V_2^2/2g + h_f \qquad (19)$$

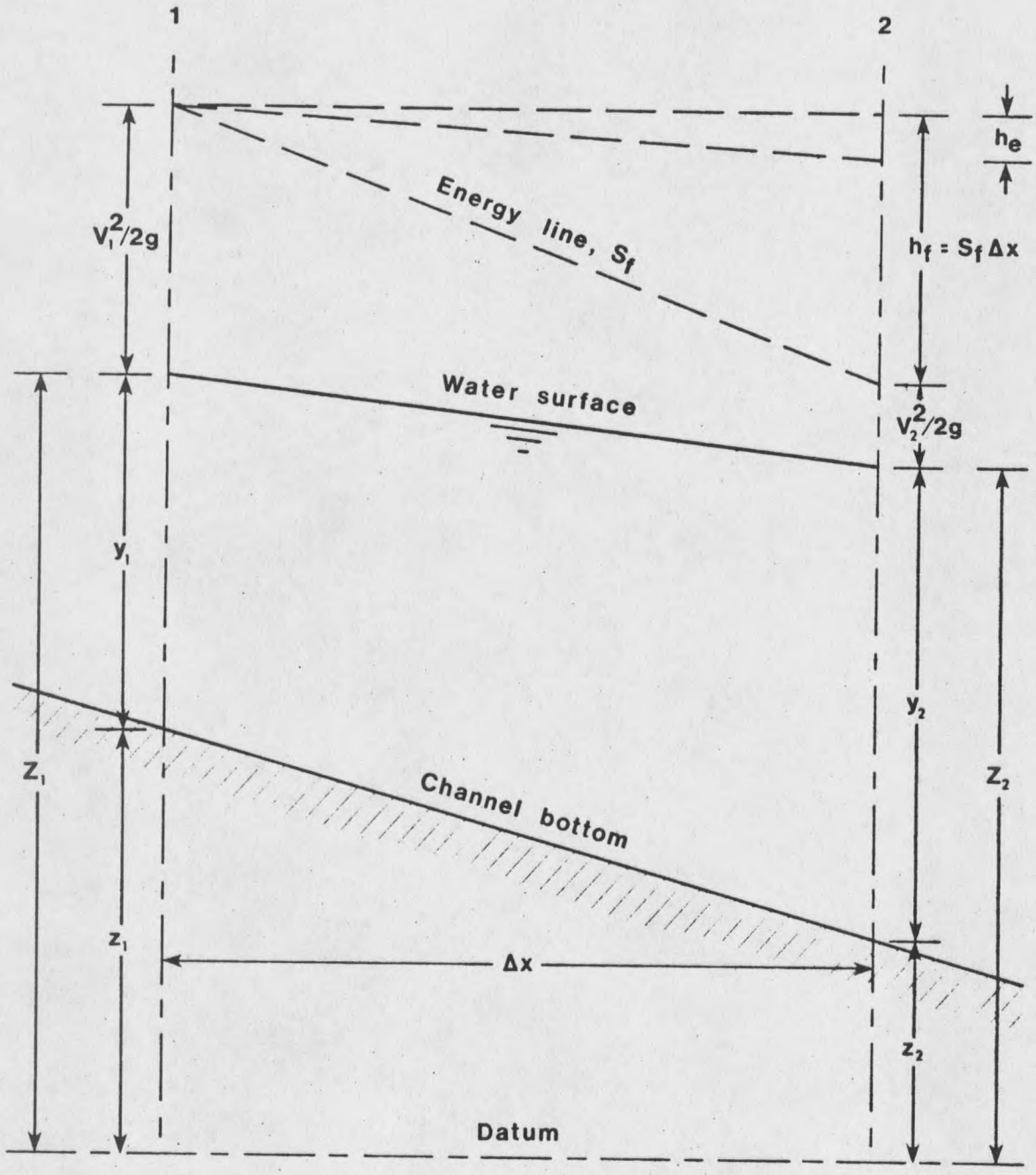

Figure 17. Longitudinal cross-section of channel length Δx to illustrate the terms in the standard step-backwater method. (From Chow, 1959).

where V_1 and V_2 are the velocities, g is the gravitational constant, h_f is the friction loss expressed as:

$$h_f = S_f \Delta x \tag{20}$$

and Z_1 and Z_2 are the water surface elevations:

$$Z_1 = y_1 + z_1 \tag{21}$$

$$Z_2 = y_2 + z_2 \tag{22}$$

where z_1 and z_2 are the channel bottom elevations.

A known depth at section 1 and a trial depth at section 2 are entered into equation 19. The depth is tested and corrected until the residual disappears. The depth y_2 then becomes the known and a new depth is solved for at the next section. The direction in which the computations are carried is governed by the regime of flow in the channel. If the flow is subcritical the computations are carried upstream; if supercritical they are carried downstream (Chow, 1959).

The calculation of the friction slope S_f, used in the backwater calculation, requires an estimate of the roughness coefficient n. Manning's n is an empirical coefficient to estimate the resistance to flow in a given channel (Chow, 1959; 1964). Furthermore, Chow (1959, p. 101) states:

> the greatest difficulty lies in the determination of the roughness coefficient n; for there is no exact method of selecting the n value. At the present stage of knowledge, to select a value of n . . . is really a matter of intangibles . . . ; for beginners, it can be no more than a guess . . .

Reasonable field estimates of Manning's n, (.045-.085), from tables contained in Chow (1959; 1964) and photo comparisons from Barnes (1967), yielded unreasonably low values for the friction slope S_f and the friction loss h_f. In a stream that has reached a steady state, i.e., the rates of import and export of material and energy are balanced (Morisawa, 1968), the friction slope can be assumed to be equal to the bed slope (D. R., Reichmuth, oral commun., 1980). By setting the initial friction slope equal to the bed slope, Manning's n is back-calculated using equation 3 for each reach of the stream. The n values for the upstream reaches are extremely high due to the steepness and irregularity of the stream bed. More energy is dissipated in a stream with a steep slope and "drop-structures" (waterfalls and pools), than in a stream with a mild, uniform slope. The increased energy loss must be accounted for in the Manning friction term (D. R., Reichmuth, oral commun., 1980).

COMPUTER REPRESENTATION OF THE MODEL

The mathematical equations from the previously described model are represented in a FORTRAN IV computer program listed in Appendix II. In order to insure the readability of the code and to retain the structure of the model, the program is divided into 3 modules or subprograms: MAINLINE, BREACH and NOAH. Each of these subprograms performs a specific task. In MAINLINE, the "housekeeping" module, all variables are read in, initial conditions are established, calls to the BREACH and NOAH subprograms are regulated, output data is generated and stored, and user information is provided concerning input and output formats as well as variable lists and definitions. The BREACH module simulates the time-dependent failure of the dam and the breach hydrograph, while NOAH routes the floodwave downstream. (NOAH was modified from a program by Amein and Fang, 1968).

In order to execute their specific assignments, each of these modules require the following subroutines and function subroutines to solve repetative or specialized calculations.

AREA - function subroutine to calculate the cross-sectional area as a function of depth.

BACKWATER - subroutine to determine the initial conditions of depth and discharge at each cross-section.

DRCDY - function subroutine to compute the derivative of the rating curve at the downstream boundary with respect to depth.

DRDY - function subroutine to take the derivative of the hydraulic radius with respect to depth.

DTWDY - function subroutine to take the derivative of the top width with respect to depth.

LAKE - subroutine to calculate the water surface elevation of the reservoir as a function of the lake volume.

MATRIX - subroutine to generate the coefficient matrix.

OUTLET - function subroutine to calculate the discharge through the outlet gates as a function of lake level.

RADIUS - function subroutine to determine the hydraulic radius of the breach.

RATING - function subroutine to calculate the discharge at the downstream boundary as a function of depth.

SIMEQ - subroutine to solve the coefficient matrix using a modified Gaussian elimination method (Gauss-Jordan) to solve the matrix in place and conserve storage space.

SPILLWAY - function subroutine to compute the discharge through the spillway as a function of the lake level.

TOPW - function subroutine to calculate the top width at each cross-section as the derivative of the cross-

sectional area with respect to depth.

VOLUME - function subroutine to determine the volume of the reservoir as a function of the reservoir depth.

WP - function subroutine to compute the wetted perimeter of the stream channel as a function of depth.

The logical progression through the program and the sequence of subroutine calls is illustrated in a flow chart in Appendix I.

Information of interest to be gained from the simulation includes the maximum values of depth, discharge, top width, water surface elevations, and the time of occurrence of these maximum values at each cross-section along the stream. In addition, a continuous record of discharge is collected at various cross-sections (to be selected by the user) for plotting hydrographs.

RESULTS

The program was tested and run successfully with data defining an imaginary stream with uniform cross-sections and a uniform bed slope. However, when the data file defining Bozeman Creek was input, the program failed to run successfully. The author believes this is due to the changes in the flow regime in Bozeman Creek.

The extreme variablity of the channel cross-sections and the bed slope of Bozeman Creek create "control sections" which regulate the flow regime. A constriction in the channel impedes the flow of water producing subcritical flow and a backwater area upstream of the constriction, and supercritical flow at the constriction. Similarly, a change in the bed slope from steep to gentle, or an expansion in the channel, alters the flow regime from super to subcritical (Chow, 1959).

These "control sections" present a problem in establishing the initial conditions of flow. In a stream where the flow regime is constant over the total length, the water surface profile may be computed by a single backwater calculation. However, with a change in the flow regime, the initial depths must be known at each "control section" and a separate backwater profile computed for each reach between the "control sections". A network of gaging stations along

Bozeman Creek may not solve the problem completely. Constrictions in the stream channel may only exert control on the flow under high water conditions. Therefore, gaging the stream under normal flow conditions may not allow realistic extrapolations for a high discharge event.

Another problem involving the changes in flow regime is the establishment of boundary conditions. Each of these "control sections" act as intermediate boundary conditions and as such require rating curves to be incorporated into the matrix solution (M. Amein, personal commun., 1981). Without the rating curves from the gaging data, this task is impossible. Because of these problems the routing portion of the model is not applicable to Bozeman Creek. Therefore the magnitude, timing and extent of flooding from the failure of the dam cannot be simulated.

However, a rough first approximation of the depth of flow at the canyon mouth can be estimated by plotting the percentage attenuation of the breach hydrograph against the depth of flow. The total conveyance K at Leverich Road is tabulated as a function of depth by the U.S. Soil Conservation Service (R., Bergantine, personal commun., 1981). For For any discharge Q, and a channel slope S of 0.01, the total conveyance can be calculated as:

$$K = Q / \sqrt{S} \qquad (23)$$

The depth corresponding to the conveyance is read from the SCS table and plotted against the percentage attenuation in figure 18. Figure 18 presents all possible cases for consideration; the worst possible--0% attenuation, and the best possible--100% attenuation. Based on the hydrographs from the Teton and Buffalo Creek dam failures, a 60 percent attenuation over the 7 miles between the dam and the canyon mouth is reasonable (Fread, 1980). A cross-sectional profile at Leverich Road (Fig. 19) illustrates the extent of flooding for all cases of attenuation. The 500 year flood is denoted in figures 18 and 19 as a reference point to indicate the magnitude of the estimated flood.

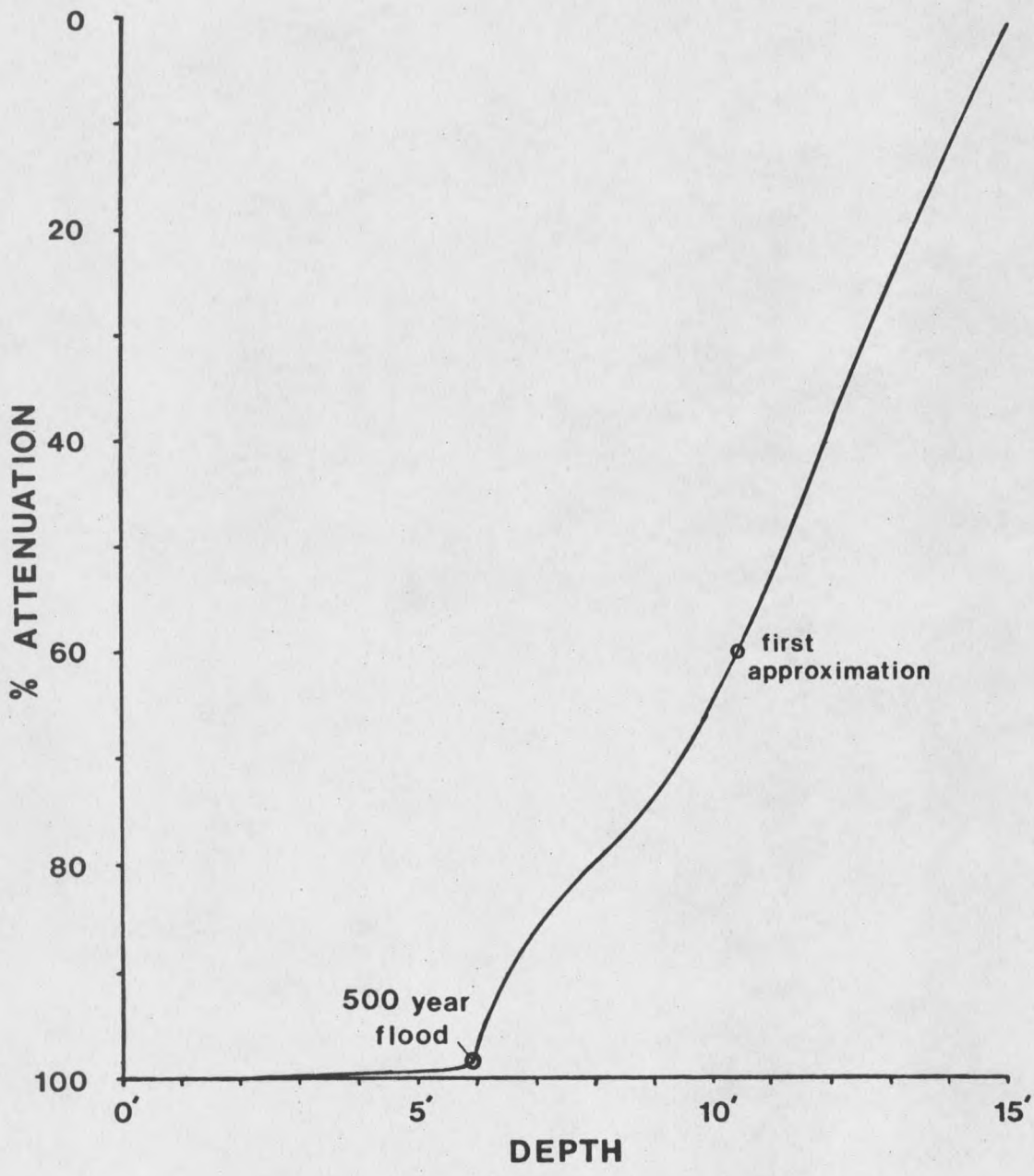

Figure 18. Depth of flow at the canyon mouth (Leverich Rd.) as a function of the percentage attenuation of the breach outflow hydrograph (Fig. 10). A 60 percent attenuation, based on previous dam failures, produces a depth of flow of 10.5 feet; 4.5 feet deeper than the 500 year flood.

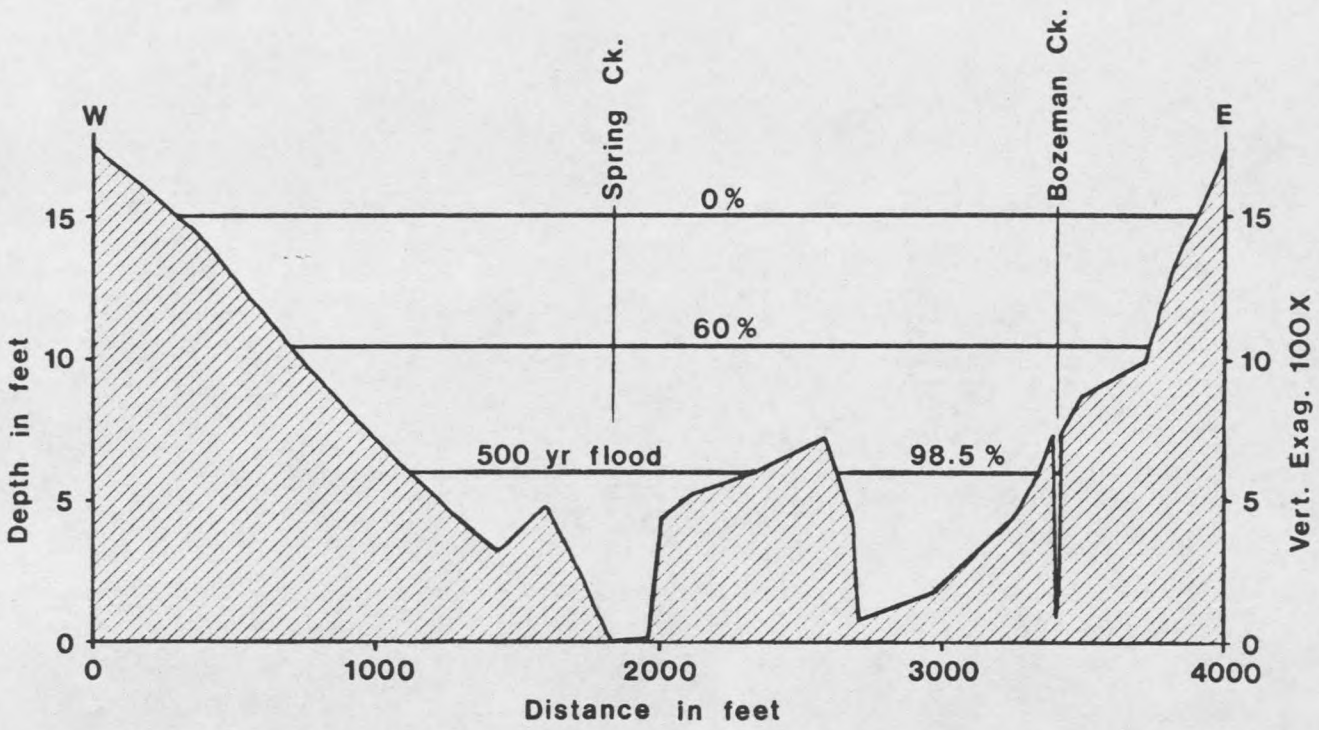

Figure 19. Cross-sectional profile at Leverich Rd. to demonstrate the extent of flooding for 3 cases of attenuation: 0% (worst possible case), 60% (first approximation), and 98.5% (500 year flood). (Profile data from R., Bergantine, personal commun., 1981).

SUMMARY AND CONCLUSIONS

1). Mystic Lake dam was constructed using engineering practices that are now outdated. Compared to modern safety requirements, the embankment slopes are overly steep. The masonry core wall is cracked and does not extend through the total length of the dam. Where the core wall is absent, water seeps through the dam and ponds in a depression at the toe of the dam. The spillway is inadequate to handle a flood with a discharge greater than 780 cfs.

2). The dam is located in a unstable geologic setting. The eastern half of the dam is founded in the toe of a recent landslide and the western abutment in weathered dolomite and friable sandstone. Pore-pressure from the seepage water ponding at the toe of the dam escalates the risk of damage from an earthquake in an already high seismic risk zone. Slump scarps present in the landslide deposit directly below the dam are attributed to the increased pore-pressure from the seepage pond. The dam is also undergoing differential settlement which has in the past lead to the failure of the outlet pipes and near failure of the dam due to piping.

3). If overtopped, the dam would fail rapidly and produce a peak discharge of 83,500 cfs, creating a severe

potential for property damage and possible loss of life.

4). The rapidly-varied flow associated with a dam-break floodwave has appreciable acceleration and frictional effects and can only be modelled by a hydraulic routing method utilizing the complete equations of unsteady flow.

5). The four-point implicit method is the best finite difference scheme for the numerical solution of the unsteady flow equations because it is unconditionally stable, not restricted to small time steps, and the distance steps need not be constant.

6). Changes in the flow regime in Bozeman Creek present insurmountable problems in establishing the initial conditions of flow and intermediate boundary conditions. Without stream gaging data, the model is not applicable to Bozeman Creek and the extent of flooding cannot be modelled.

7). A first approximation of the extent of flooding can be achieved by plotting the depth of flow against the percentage attenuation of the breach hydrograph. A 60% attenuation yields a depth of flow of 10.5 feet at the canyon mouth, 4.5 feet deeper than the 500 year flood.

REFERENCES CITED

REFERENCES CITED

Abbott, M. B., 1975, Method of characteristics, in Mahmood, K., and Yevjevich, V., eds., Unsteady flow in open channels: Ft. Collins, Colo., Water Res. Pub., p. 63-88.

Abbott, M. B., and Ionescu, F., 1967, On the numerical computation of nearly horizontal flows: Jour. Hydraulic Research., v. 5, no. 2, p. 97-117.

Algermissen, S. T., and Perkins, D. M., 1976, A probabilistic estimate of maximum accelerations in rock in the contiguous United States: U.S. Geol. Survey Bull., Open File Report 76-416.

Amein, M., 1967, Some recent studies on numerical flood routing: 3rd Annual Conf., Am. Water Resources Assoc., San Francisco, Calif., 1967, Proc. p. 274-284.

-----1968, An implicit method for numerical flood routing: Water Res. Research, AGU, v. 4, no. 4, p. 719-726.

-----1975, Comparison of four numerical methods for flood routing: Jour. Hydraulic Div., Am. Soc. Civ. Eng., v. 101, no. HY8, p. 1098-1099.

Amein, M., and Fang, C. S., 1969, Streamflow routing (with application to North Carolina Rivers): Raliegh, N.C., Water Res. Research Inst. N.C. State Univ., no. 17, 72 p.

-----1970, Implicit flood routing in natural channels: Jour. Hydraulic Div., Am. Soc. Civ. Eng., v. 96, no. HY12, p. 2481-2500.

Amein, M., and Chu, H. L., 1975, Implicit numerical modelling of unsteady flows: Jour. Hydraulic Div., Am. Soc. Civ. Eng., v. 101, no. HY6, p. 717-731.

American Society of Civil Engineers, 1975, Lessons from dam incidents, U.S.A.: New York, Am. Soc. Civ. Eng., 387 p.

Aram, R. B., 1979, Cenozoic geomorphic history relating to Lewis and Clark Caverns, Montana (Masters thesis): Mont. State Univ., Bozeman, Mont., 150 p.

Bailey, J. F., and Ray, H. A., 1966, Definition of stage-discharge relation in natural channels by step-back-water analysis: U.S. Geol. Survey Water Supply Paper 1869-A, 24 p.

Balloffet, A., Cole, E., and Balloffet, A. F., 1974, Dam collapse wave in a river: Jour. Hydraulic Div., Am. Soc. Civ. Eng., v. 100, no. HY5, p. 645-665.

Baltzer, R. A., and Lai, C., 1968, Computer simulations of unsteady flows in waterways: Jour. Hydraulic Div., Am. Soc. Civ. Eng., v. 94, no. HY4, p. 1083-1117.

Barnes, H. H., 1967, Roughness characteristics of natural channels: U.S. Geol. Survey Water-Supply Paper 1849, 213 p.

Barron, R. A., 1977, The design of earth dams, in Golze', A. R., ed., Handbook of dam engineering: New York, Van Nostrand Reinhold, p. 291-318.

Brakensiek, D. L., 1966, Finite difference methods: Water Res. Research, AGU, v. 3, no. 3, p. 847-860.

Brakensiek, D. L., and Comer, G. H., 1965, A re-examination of a flood routing method comparison: Jour. of Hydrology, v. 1, no. 3, p. 223-230.

CH2M Hill, 1980, Phase 1 inspection report, national dam safety program, Mystic Lake dam, Bozeman, Montana, MT-880: unpublished report, 70 p.

Chadwick, R. A., 1970, Belts of eruptive centers in the Absaroka-Gallatin volcanic province, Wyoming-Montana: Geol. Soc. America Bull., v. 81, p. 267-274.

Chaudhry, Y. M., and Contractor, D. N., 1973, Application of the implicit method to surges in open channels: Water Res. Research, AGU, v. 9, no. 6, p. 1605-1612.

Chow, V. T., 1959, Open channel hydraulics: New York, McGraw Hill, 680 p.

-----ed., 1964, Handbook of applied hydrology--a compendium of water-resources technology: New York, McGraw-Hill, 1453 p.

Cunge, J. A., 1975, Applied mathematical modelling of open channel flow, in Mahmood, K., and Yevjevich, V. M., eds., Unsteady flow in open channels: Ft. Collins, Colo., Water Res. Pub., p. 379-404.

De Saint-Venant, B., 1871, Theory of unsteady water flow, with application to river floods and to propagation of tides in river channels: Acad. Sci. (Paris), v. 73, p. 237-240.

Dressler, R. F., 1954, Comparison of theories and experiments for the hydraulic dam-break wave: Internat. Assoc. Sci. Pubs., v. 3, no. 38, p. 319-328.

Fread, D. L., 1971, Discussion of implicit flood routing in natural channels (Amein and Fang, 1971): Jour. Hydraulic Div., Am. Soc. Civ. Eng., v. 97, no. HY7, p. 1156-1159.

-----1974a, Numerical properties of implicit four-point finite difference equations of unsteady flow: NOAA Tech. Memo. NWS Hydro-18, U.S. Dept. of Commerce, Nat'l Oceanic and Atmos. Admin., Nat'l Weather Ser., p. 38.

-----1978, The National Weather Service dam-break flood forecasting model: Dam-Break Modelling Seminar, Portland, Oregon, 1978, Proc., 37 p.

Fread, D. L., and Harbaugh, T. E., 1973, Transient simulation of breached earth dams: Jour. Hydraulic Div., Am. Soc. Civ. Eng., v. 99, no. HY1, p. 139-154.

Gilcrest, B. R., 1950, Flood routing, in Rouse, H., ed., Engineering hydraulics: New York, Wiley, p. 635-710.

Glass, R. W., Keefer, T. N., and Rankl, J. G., 1976, Hydrologic effects of hypothetical earthquake-caused floods below Jackson Lake, NW Wyoming: U.S. Geol. Survey Water Res. Inv. / Open-File Report 76-77, 32 p.

Greco, F., and Panattoni, L., 1975, An implicit method to solve Saint-Venant equations: Jour. of Hydrology, v. 24, p. 171-185.

Gundlach, D. L., and Thomas, W. A., 1977, Guidelines for calculating and routing a dam-break flood: U.S. Army Corps of Eng., Res. Note No. 5, 41 p.

Housner, G. W., 1977, Earthquake hazard, in Golze', A. R., ed., Handbook of dam engineering: New York, Van Nostrand Reinhold, p. 246-266.

Hughes, G. C., 1980, Cenozoic geology and geomorphology of the Dry Creek Valley, Gallatin County, Montana (Masters thesis): Mont. State Univ., Bozeman, Mont., 146 p.

James, M. L., Smith, G. M., and Wolford, J. C., 1977., Applied numerical methods for digital computation with FORTRAN and CSMP (2d ed.): New York, Harper and Row, 687 p.

Kirkpatrick, G. W., 1977, Evaluation guidelines for spillway adequacy: The Evaluation of Dam Safety, Eng. Foundation Conf., Am. Soc. Civ. Eng., New York, 1977, Proc., p. 395-414.

Liggett, J. A., 1975, Basic equations of unsteady flow, in Mahmood, K., and Yevjevich, V. M., eds., Unsteady flow in open channels: Ft. Collins, Colo., Water Res. Pub., p. 29-62.

Liggett, J. A., and Cunge, J. A., 1975, Numerical methods of solution of the unsteady flow equations, in Mahmood, K., and Yevjevich, V. M., eds., Unsteady flow in open channels: Fort Collins, Colo., Water Res. Pub., p. 89-182.

Liggett, J. A., and Woolhiser, D. A., 1967, Difference solution of the shallow-water equations: Jour. Eng. Mech. Div., Am. Soc. Civ. Eng., v. 98, no. EM2, p. 39-71.

McMannis, W. J., 1955, Geology of the Bridger Range Montana: Geol. Soc. America Bull., v. 66, no. 11, p. 1385-1430.

Middlebrooks, T. A., 1953, Earth-dam practice in the U.S. : Centennial Trans., Am. Soc. Civ. Eng., v. CT, no. 2620, p. 697-722.

Miller, W. A., and Cunge, J. A., 1975, Simplified equations of unsteady flow, in Mahmood, K., and Yevjevich, V. M., eds., Unsteady flow in open channels: Ft. Collins, Colo., Water Res. Pub., p. 183-249.

Miller, W. A., and Woolhiser, D. A., 1975, Choice of models, in Mahmood, K., and Yevjevich, V. M., eds., Unsteady flow in open channels: Ft. Collins, Colo., Water Res. Pub., p. 367-377.

Morisawa, M., 1968, Streams--their dynamics and morphology: New York, McGraw-Hill, 175 p.

Northern Testing Laboratories, 1977, Report of leakage investigation, Mystic Lake dam, Bozeman, Montana, in CH2M Hill, 1980, Appendix 2, Phase 1 inspection report, national dam safety program, Mystic Lake dam, Bozeman, Montana, MT-880: unpublished report, p. 27-44.

Ponce, V. M., Indlekoff, H., and Simons, D. B., 1978, Convergence of the four-point implicit water wave models : Jour. Hydraulic Div., Am. Soc. Civ. Eng., v. 104, no. HY7, p. 947-958.

Price, R. K., 1974, Comparison of four numerical methods for flood routing: Jour. Hydraulic Div., Am. Soc. Civ. Eng., v. 100, no. HY7, p. 879-899.

Rao, V. S., Contractor, D. N., and Tiyamani, C., 1976, Optimal river cross sections for flood routing: Symposium on Inland Waterways, Am. Soc. Civ. Eng., 1976, Proc., p. 421-433.

Rajar, R., 1978, Mathematical simulation of dam-break flow: Jour. Hydraulic Div., Am. Soc. Civ. Eng., v. 104, no. HY7, p. 1011-1026.

Richtmyer, R. D., 1962, A survey of difference methods for non-steady fluid dynamics: Natl. Center for Atmos. Research, Boulder, Colo., Tech. note 63-2.

Roberts, A. E., 1964a, Geologic map of the Fort Ellis quadrangle, Montana: U.S. Geol. Survey, Misc. Geol. Inv. Map I-397.

-----1964b, Geologic map of the Mystic Lake quadrangle, Montana: U.S. Geol. Survey, Misc. Geol. Inv. Map I-398.

Sakkas, J. G., and Strelkoff, T., 1973, Dam break flood in a prismatic dry channel, Jour. Hydraulic Div., Am. Soc. Civ. Eng., v. 99, no. HY12, p. 2195-2216.

Seed, B. H., 1973, Stability of earth and rockfill dams during earthquakes, in Hirchfeld, R. C., and Poulos, S. J., eds., Embankment-dam engineering (Casagrande Vol.): New York, Wiley, p. 239-269.

Sherard, J. L., 1973, Embankment dam cracking, in Hirchfeld, R. C., and Poulos, S. J., eds., Embankment-dam engineering (Casagrande Vol.): New York, Wiley, p. 271-353.

Sherard, J. L., Woodward, R. J., Gizienski, S. F., and Clevenger, W. A., 1963, Earth and earth-rock dams; engineering problems of design and construction: New York, Wiley, 725 p.

Sowers, G. F., 1962, Earth and rockfill dam engineering: New York, Asia Publishing House, 283 p.

Stoker, J. J., 1948, The formation of breakers and bores: Comm. on Pure and Applied Math., v. 1, p. 1-87.

-----1957, Water waves: New York, Inter-science, 507 p.

Strelkoff, T., 1970, Numerical solution of Saint-Venant equations: Jour. Hydraulic Div., Am. Soc. Civ. Eng., v. 96, no. HY1, p. 223-252.

Su, S. T., and Barnes, A. H., 1970, Geometric and frictional effects on sudden releases: Jour. Hydraulic Div., Am. Soc. Civ. Eng., v. 96, no. HY11, p. 2185-2200.

Thomas, H. A., 1934, The hydraulics of flood movements in rivers: Pittsburg, Penn., Carnegie Inst. of Tech., 70 p.

Tracy, H. J., 1957, Discharge characteristics of broad-crested weirs: U.S. Geol. Survey Circ. 397, 15 p.

U.S. Army Corps of Engineers, 1957, Flow through a breached dam: U.S. Army Corps of Eng., Mil. Hydro. Bull., v. 9.

U.S. Army Corps of Engineers, 1960, Floods resulting from suddenly breached dams--conditions of minimum resistance, hydraulic model investigation: Misc. Paper 2-374 Report 1, 176 p.

U.S. Army Corps of Engineers, 1961, Floods resulting from suddenly breached dams--conditions of maximum resistance, hydraulic model investigation: Misc. Paper 2-374 Report 2, 121 p.

U.S. Army Corps of Engineers, 1975, National program of inspection of dams: Washington D. C., Dept. of the Army, v. I-V.

U.S. Bureau of Reclamation, 1974, Design of small dams (2nd ed.): U.S. Dept. of Interior, Water Res. Tech. Pub., 816 p.

U.S. Department of Agriculture, Soil Conservation Service, 1972, East Gallatin River and upper tributaries flood hazard analyses, Gallatin County, Montana: Bozeman, Montana, U.S. Dept. of Agriculture, SCS, 112 p.

U.S. Department of Agriculture, Soil Conservation Service, 1979, Simplified dam-break routing procedure: Technical Release No. 66, 36 p.

U.S. Department of Agriculture, Soil Conservation Service, 1980, Preliminary investigation report, Bozeman Creek watershed, Gallatin County, Montana: Bozeman, Montana, U.S. Dept. of Agriculture, SCS, 37 p.

Van't Hul, A., 1979, Summary of design and construction history of Mystic Lake dam, in CH2M Hill, 1980, Appendix 1 Phase 1 inspection report, national dam safety program, Mystic Lake dam, Bozeman, Montana, MT-880: unpublished report, p. 20-26.

Vasiliev, O. F., 1970, Numerical solution on the non-linear problems of unsteady flow in open channels: 2nd Inter. Conf. on Numerical Methods in Fluid Dynamics, Berkeley, Calif., 1970, Proc., p. 410-422.

Vasiliev, O. F., Voyevodin, A. F., and Atavin, A. A., 1976, Numerical methods for calculation of unsteady flow in systems of open channels and canals: Symposium on unsteady flow, Newcastle-upon-Tyne, England, 1976, Proc. p. E2-15 - E2-22.

Whitman, G. B., 1955, The effects of hydraulic resistance in the dam-break problem: Royal Soc. London, v. 227, p. 399-407.

Williams, T. T., 1959, Report on Mystic Lake for the Bozeman Creek Reservoir Association: unpublished report, 13 p.

-----1977, Sinkhole inspection report for the Bozeman Creek Reservoir Association, in CH2M Hill, 1980, Appendix 3, Phase 1 inspection report, national dam safety program, Mystic Lake dam, Bozeman, Montana, MT-880: unpublished report, p. 45-50.

Wilson, S. D., and Marsal, R. J., 1979, Current trends in design and construction of embankment dams: New York, Am. Soc. Civ. Eng., 125 p.

Yevjevich, V. M., 1964, Bibliography and discussion of flood routing methods and unsteady flow in channels: U.S. Geol. Survey Water Supply Paper 1690, 235 p.

-----1975, Sudden water release, in Mahmood, K., and Yevjevich, V. M., eds., Unsteady flow in open channels: Fort Collins, Colo., Water Res. Pub., p. 587-665.

Zeigler, B. P., 1976, Theory of modelling and simulation: New York, Wiley, 435 p.

APPENDICES

APPENDIX I
PROGRAM FLOW CHART

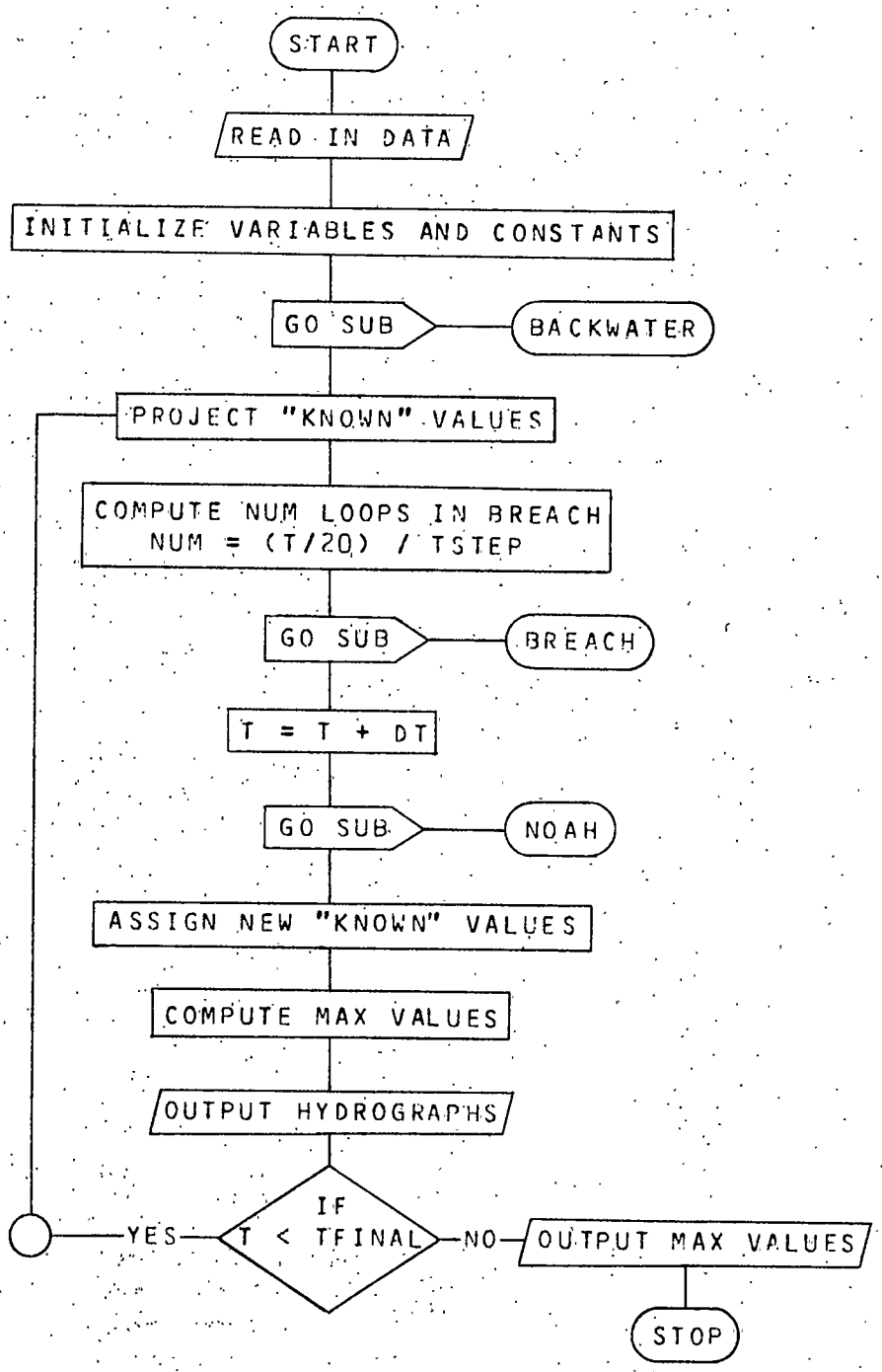

APPENDIX II
PROGRAM LISTING

```
C*****************************************************************
C
C     MAINLINE PROGRAM
C
C HOUSEKEEPING MODULE TO INITIALIZE CONDITIONS AND REGULATE
C CALLS TO THE BREACH AND NOAH SUBPROGRAMS.
C
      COMMON/ARRAY/A(200,200),N
      COMMON/BREACHS/NUM,TSTEP,LO,L1,L2,DEPTH,BD,HDAM,
     * AREAB,FLAG,INLAKE,TQ1,VOL,MNB,TFAIL
      COMMON/PARAMETERS/Y(100,2),Q(100,2),Z(100),MN(100),
     * INFLO(100),DIST(100),QMAX(100),YMAX(100),TMAX(100),
     * XSEC(5),DT,T
      COMMON/COEFS/AC1(100),AC2(100),AC3(100),RC1,RC2,RC3
      COMMON/CONSTANTS/G,TFINAL,THETA,VN,QTOL,YTOL
      REAL LAKE,LO,L1,L2,INFLO,MNB,INLAKE,MN
      INTEGER FLAG,XSEC
C
C*****************************************************************
C
C USER INFORMATION:
C
C*****************************************************************
C
C SUBROUTINES REQUIRED
C     MAINLINE      -     BREACH      -     NOAH
C
C     BACKWATER           LAKE              MATRIX
C                                           SIMEQ
C
C*****************************************************************
C
C FUNCTION SUBROUTINES REQUIRED
C     MAINLINE      -     BREACH      -     NOAH
C
C     OUTLET()            OUTLET()          AREA()
C     SPILLWAY()          RADIUS()          DRCDY()
C     VOLUME()            SPILLWAY()        DRDY()
C                         VOLUME()          DTWDY()
C                                           RATING()
C                                           RCY()
C                                           TOPW()
C                                           WP()
C
```

```
C*****************************************************************
C
C INPUT FORMAT:
C
C       THE INPUT WILL BE DISCUSSED IN TWO SECTIONS, ONE FOR
C EACH SUBPROGRAM - BREACH AND NOAH.  ALL INPUT WILL BE READ
C IN IN AN 'F' FORMAT UNLESS SPECIFIED OTHERWISE.  THE 'F'
C FORMAT CONTROL REQUIRES ONLY THAT THE DATA BE SEPERATED BY
C COMMAS OR SPACES.  EITHER REAL OR INTEGER VALUES CAN BE
C READ IN WITH NO OTHER FORMATTING SPECIFICATIONS.
C     EG. 3.506,15,0.1763E-22,5
C
C*****************************************************************
C
C BREACH VARIABLES
C
C  VARIABLE                        DEFINITION
C
C    AREAB     = BREACH AREA
C    AREAF     = EFFECTIVE AREA OF BREACH FLOW
C    BD        = BREACH DEPTH AT EACH TIME STEP
C    BQ        = DISCHARGE THRU THE BREACH
C    DEPTH     = INITIAL LAKE DEPTH
C    DL        = CHANGE IN LAKE LEVEL FROM THE LAST TIME STEP,
C                USED AS A CORRECTOR TO PROJECT THE CHANGE IN
C                LAKE LEVEL FOR THE NEXT TIME STEP
C    DT        = CHANGE IN TIME PER 'NUM' LOOPS THRU BREACH
C    ED        = DEPTH OF FLOW IN THE BREACH CHANNEL
C    HDAM      = DAM HEIGHT (48 FEET)
C    INLAKE    = INFLOW INTO THE LAKE (CFS)
C    L0        = LAKE LEVEL AT THE TIME STEP T-2
C    L1        = LAKE LEVEL AT THE TIME STEP T-1
C    L2        = LAKE LEVEL CALCULATED AT PRESENT TIME STEP T
C    LDUM      = PROJECTED LAKE LEVEL FOR PRESENT TIME STEP T
C    MNB       = MANNING'S N FOR THE BREACH CHANNEL
C    NUM       = NUMBER OF LOOPS THRU BREACH FOR EVERY CALL TO
C                NOAH
C    SLOPE     = FRICTION SLOPE OF THE BREACH CHANNEL
C    T         = TIME STEP COUNTER
C    TFAIL     = ESTIMATED TIME OF FAILURE
C    TQ1       = SUM DISCHARGE FROM THE SPILLWAY, OUTLETS,
C                AND BREACH (CFS) - START OF EACH CALL TO THE
C                BREACH SUBROUTINE
C    TQ2       = SUM DISCHARGE FROM THE SPILLWAY, OUTLETS,
C                AND BREACH (CFS) - AFTER 'NUM' LOOPS IN THE
C                BREACH SUBROUTINE
```

```
C    TSTEP     = TIME STEP INCREMENT (seconds)
C    TZERO     = STARTING TIME FOR EACH CALL TO BREACH
C    VOL       = VOLUME OF THE LAKE
C
*****************************************************************
C
C BREACH DATA REQUIREMENTS:
C
C    CARD OR RECORD 1: COMMENT CARD (SEE EXAMPLE DATA)
C    CARD OR RECORD 2: INITIAL CONDITIONS OF THE BREACH
      READ(105,1) DEPTH,INLAKE,TSTEP,MNB,TFAIL
    1 FORMAT(/,5(F))
C
*****************************************************************
C
C INITIALIZE BREACH CONSTANTS AND VARIABLES
      T=FLAG=0.0
      HDAM=48.0
      L0=L1=DEPTH
      VOL=VOLUME(DEPTH)
      BD=0.0
      TQ1=SPILLWAY(DEPTH) + OUTLET(DEPTH)
C
*****************************************************************
C
C NOAH VARIABLES
C
C  VARIABLE                    DEFINITION
C
C    AA(I,J)   = COEFFICIENT MATRIX
C    A1        = AREA AT NODE  I,J
C    A2        = AREA AT NODE  I,J+1
C    A3        = AREA AT NODE  I+1,J
C    A4        = AREA AT NODE  I+1,J+1
C    AC1,2,3   = COEFFICIENTS OF THE DEPTH-AREA CURVE AT EACH
C                X-SECTION
C    AVA       = AVERAGE AREA BETWEEN A2 AND A4
C    AVR       = AVERAGE HYDRAULIC RADIUS BETWEEN R2 AND R4
C    AVQ       = AVERAGE DISCHARGE BETWEEN Q2 AND Q4
C    DIST(I)   = DISTANCE BETWEEN NODES I AND I+1
C    DQ        = CHANGE IN DISCHARGE
C    DQDT      = CHANGE IN DISCHARGE WITH CHANGE IN TIME
C    DQDX      = CHANGE IN DISCHARGE WITH CHANGE IN DISTANCE
C    DT        = CHANGE IN TIME (TIME STEP)
C    DTDX      = CHANGE IN TIME WITH CHANGE IN DISTANCE
C    DXDT      = CHANGE IN DISTANCE WITH CHANGE IN TIME
```

```
C     DY          = CHANGE IN DEPTH
C     DYDT        = CHANGE IN DEPTH WITH CHANGE IN TIME
C     DYDX        = CHANGE IN DEPTH WITH CHANGE IN DISTANCE
C     G           = GRAVITATIONAL CONSTANT
C     INFLO(I)    = LATERAL INFLOW ALONG CHANNEL LENGTH DX(I)
C     MN(I)       = MANNING'S N FOR EACH REACH
C     PEAKT       = TIME OF ARRIVAL OF THE PEAK
C     PCEQ2       = PARTIAL DERIVATIVE OF THE CONTINUITY EQUATION
C                   WITH RESPECT TO Q2
C     PCEQ4       = PARTIAL DERIVATIVE OF THE CONTINUITY EQUATION
C                   WITH RESPECT TO Q4
C     PCEY2       = PARTIAL DERIVATIVE OF THE CONTINUITY EQUATION
C                   WITH RESPECT TO Y2
C     PCEY4       = PARTIAL DERIVATIVE OF THE CONTINUITY EQUATION
C                   WITH RESPECT TO Y4
C     PMEQ2       = PARTIAL DERIVATIVE OF THE MOMENTUM EQUATION
C                   WITH RESPECT TO Q2
C     PMEQ4       = PARTIAL DERIVATIVE OF THE MOMENTUM EQUATION
C                   WITH RESPECT TO Q4
C     PMEY2       = PARTIAL DERIVATIVE OF THE MOMENTUM EQUATION
C                   WITH RESPECT TO Y2
C     PMEY4       = PARTIAL DERIVATIVE OF THE MOMENTUM EQUATION
C                   WITH RESPECT TO Y4
C     Q1          = DISCHARGE AT NODE  I,J
C     Q2          = DISCHARGE AT NODE  I,J+1
C     Q3          = DISCHARGE AT NODE  I+1,J
C     Q4          = DISCHARGE AT NODE  I+1,J+1
C     QMAX(I)     = MAXIMUM DISCHARGE AT EACH X-SECTION
C     QTOL        = TOLERANCE LIMIT FOR ERROR IN DISCHARGE (50.0
C                   CFS)
C     R2          = HYDRAULIC RADIUS AT NODE  I,J+1
C     R4          = HYDRAULIC RADIUS AT NODE  I+1,J+1
C     RC1,2,3     = COEFFICIENTS OF THE DOWNSTREAM RATING CURVE
C     RCE         = RESIDUAL OF THE CONTINUITY EQUATION
C     RESY        = DEPTH RESIDUAL
C     RESQ        = DISCHARGE RESIDUAL
C     RME         = RESIDUAL OF THE MOMENTUM EQUATION
C     SF          = FRICTION SLOPE TERM
C     SLOPE       = WATER SURFACE SLOPE
C     T           = TIME STEP COUNTER
C     TFINAL      = TIME FOR TERMINATION
C     THETA       = WEIGHTING COEFFICIENT
C     TMAX(I)     = TIME OF PEAK EVENT AT EACH X-SECTION
C     TW2         = TOP WIDTH AT NODE I,J+1
C     TW4         = TOP WIDTH AT NODE I+1,J+1
C     XSEC(L)     = X-SECTIONS AT WHICH HYDROGRAPHS ARE GENERATED
```

```
C    Y1          = DEPTH AT NODE  I,J
C    Y2          = DEPTH AT NODE  I,J+1
C    Y3          = DEPTH AT NODE  I+1,J
C    Y4          = DEPTH AT NODE  I+1,J+1
C    YMAX(I)     = MAXIMUM DEPTH AT EACH X-SECTION
C    YTOL        = TOLERANCE LIMIT FOR ERROR IN DEPTH (.05 FEET)
C    Z(I)        = CHANNEL BOTTOM ELEVATION AT EACH X-SECTION
C
*****************************************************************
C
C NOAH DATA REQUIREMENTS:
C
C    CARD OR RECORD 3: COMMENT CARD (SEE EXAMPLE DATA)
C    CARD OR RECORD 4: ROUTING CONSTANTS FOR NOAH
      READ(105,1) N,TFINAL,THETA,QTOL,YTOL
C
C    CARD OR RECORD 5: X-SECTIONS FOR HYDROGRAPHS (LIMIT=4)
C    XSEC(1)=DAMSITE
      READ(105,2)(XSEC(I),I=2,5)
    2 FORMAT(4(F))
C
C    CARD OR RECORD 6: COMMENT CARD (SEE EXAMPLE DATA)
C    CARDS OR RECORDS 7 - N+7: VARIABLES AT EACH NODE
      READ(105,3)(Z(I),DIST(I),INFLO(I),I=1,N)
    3 FORMAT(/,3(F))
C
C    CARD OR RECORD N+8: COEFFICIENTS OF THE DOWNSTREAM
C    RATING CURVE
      READ(105,4) RC1,RC2,RC3
    4 FORMAT(3(F))
C
C    CARDS OR RECORDS N+9 - 2N+9: DEPTH-AREA COEFFICIENTS
      READ(105,4)(AC1(I),AC2(I),AC3(I),I=1,N)
C
*****************************************************************
C
C INITIALIZE NOAH CONSTANTS AND VARIABLES
      G=32.2
      NN=2*N
      XSEC(1)=1
C
C COMPUTE THE INITIAL VALUES OF DEPTH AND DISCHARGE AT EACH
C CROSS SECTION
      CALL BACKWATER
C
C SET THE MAX VALUES TO ZERO
```

```
      DO 5 I=1,N
      QMAX(I)=YMAX(I)=TMAX(I)=0.0
    5 CONTINUE
C
C*************************************************************
C
C START THE SIMULATION
C
C TEST RUN TIME
    6 IF(T.GE.TFINAL) GO TO 11
C
C PROJECT THE VALUES AT THIS TIME STEP TO THE NEXT STEP
      DO 7 I=1,N
      Q(I,2)=Q(I,1)
      Y(I,2)=Y(I,1)
    7 CONTINUE
C
C COMPUTE "NUM" LOOPS IN BREACH AS A FUNCTION OF THE ARRIVAL
C TIME OF THE WAVE.  WHEN T > TFAIL, THE TIME OF ARRIVAL OF
C THE PEAK AT ANY CROSS-SECTION IS EQUAL TO THE PRESENT
C TIME.  T IS TREATED AS THE PEAK ARRIVAL TIME.
C
      PEAKT=T
      IF(PEAKT.LT.TFAIL) PEAKT=TFAIL
      NUM = (PEAKT/20.0)/TSTEP +.5
C
C CALCULATE THE NEW OUTFLOW FROM THE BREACH
      CALL BREACH
C
C ROUTE THE FLOODWAVE DOWNSTREAM
      CALL NOAH
C
C RE-ASSIGN "KNOWN" VALUES FOR THE NEXT TIME STEP
      DO 8 I=1,N
      Q(I,1)=Q(I,2)
      Y(I,1)=Y(I,2)
    8 CONTINUE
C
C TEST FOR MAX DEPTH AND DISCHARGE AND SET TIMES OF PEAK
      DO 9 I=1,N
      IF(Y(I,2).GT.YMAX(I)) YMAX(I)=Y(I,2); TMAX(I)=T-DT
      IF(Q(I,2).GT.QMAX(I)) QMAX(I)=Q(I,2); TMAX(I)=T-DT
    9 CONTINUE
C
C OUTPUT DATA FOR HYDROGRAPHS AT SELECTED X-SECTIONS
      WRITE(101,10) T,(Q(XSEC(L),2),L=1,5)
```

```
   10 FORMAT(6F9.1)
C
C LOOP THRU AGAIN IF TFINAL HAS NOT BEEN REACHED
      GO TO 6
C
C*************************************************************
C
C OUTPUT FINAL RESULTS
   11 WRITE(108,12)
   12 FORMAT(//'STATION  MAX-DEPTH  SURF-ELEV  TOP WIDTH  ',
     *' MAX-Q   PEAK-TIME'/)
      WRITE(108,13)(I,YMAX(I),Z(I)+YMAX(I),TOPW(YMAX(I),I)
     * ,QMAX(I),TMAX(I),I=1,N)
   13 FORMAT(3X,I3,5(F10.1))
C
      END
```

```
*****************************************************************
C
      SUBROUTINE BACKWATER
C
C SUBROUTINE TO CALCULATE THE INITIAL CONDITIONS OF FLOW
C (DEPTH AND DISCHARGE) AT EACH CROSS SECTION.  A STANDARD
C STEP-BACKWATER METHOD IS UTILIZED.
C
      COMMON/ARRAY/A(200,200),N
      COMMON/BREACHS/NUM,TSTEP,L0,L1,L2,DEPTH,BD,HDAM,
     * AREAB,FLAG,INLAKE,TQ1,VOL,MNB,TFAIL
      COMMON/PARAMETERS/Y(100,2),Q(100,2),Z(100),MN(100),
     * INFLO(100),DIST(100),QMAX(100),YMAX(100),TMAX(100),
     * XSEC(5),DT,T
      COMMON/CONSTANTS/G,TFINAL,THETA,VN,QTOL,YTOL
      REAL INFLO,MN
C
*****************************************************************
C
C INITIALIZE THE UPSTREAM CONDITIONS BETWEEN THE DAM AND X-
C SECTION NUMBER ONE
C
C DISCHARGE AND DEPTH
      QDAM = SPILLWAY(DEPTH) + OUTLET(DEPTH)
      Q(1,1) = QDAM
      YDAM = DEPTH - 42.1
      Y(1,1) = YDAM
C
C ELEVATIONAL HEAD
      HU = 6396.0+YDAM
    1 HD = Z(1)+Y(1,1)
C
C VELOCITY HEAD
      VHU = (QDAM/(YDAM*20.))/(2.0*G)
      VHD = (Q(1,1)/AREA(Y(1,1),1))/(2.0*G)
C
C FRICTION SLOPE
      SF = 6396.0 - Z(1)
C
C CALCULATE RESIDUAL FROM USING Y(1,1)
      RESID = (HU+VHU) - (HD+VHD+SF)
C
C TEST THE RANGE OF THE RESIDUAL
      IF(RESID.GT.0.01)Y(1,1)=Y(1,1)+RESID;GO TO 1
      IF(RESID.LT.-0.01)Y(1,1)=Y(1,1)+RESID;GO TO 1
C
```

```
C COMPUTE THE INITIAL CONDITIONS AT EACH CROSS SECTION
      DO 3 I=1,N-1
      ITER=1
C
C DISCHARGE
      QU = Q(I,1)
      QD = Q(I+1,1)=QU+INFLO(I)
C
C DEPTH (YD IS A TRIAL VALUE THAT IS CHANGED EACH ITERATION)
      YU = Y(I,1)
      YD = YU
C
C RESTART NEXT ITERATION
    2 CONTINUE
      IF(ITER.GT.20) OUTPUT'FAILS TO CONVERGE AT',I+1; STOP

C
C STAGE
      HU = Z(I) + YU
      HD = Z(I+1) + YD
C
C AREAS
      AU=AREA(YU,I)
      AD=AREA(YD,I+1)
C
C HYDRAULIC RADII
      RU=AU/WP(YU,I)
      RD=AD/WP(YD,I+1)
C
C COMPUTE MANNING'S N FOR EACH REACH ASSUMING THE FRICTION
C SLOPE IS EQUAL TO THE BED SLOPE.
      SF=(Z(I)-Z(I+1))/DIST(I)
      MN(I)=(1.49*((AU+AD)/2.0)*((RU+RD)/2.0)**.67*(SF
     * **.5))/((QU+QD)/2.0)
C
C CALCULATE THE VELOCITY HEAD TERM
      VHU = (QU/AU)**2/(2.0*G)
      VHD = (QD/AD)**2/(2.0*G)
C
C CALCULATE THE RESIDUAL FROM USING YD
      RESID = (HU+VHU) - (HD+VHD+SF)
C
C TEST THE RANGE OF THE RESIDUAL
      IF(RESID.GT.0.01)YD=YD+RESID;ITER=ITER+1;GO TO 2
      IF(RESID.LT.-0.01)YD=YD+RESID;ITER=ITER+1;GO TO 2
C
```

```
C ASSIGN FINAL DEPTH VALUE
      Y(I+1,1) = YD
C
    3 CONTINUE
C
C OUTPUT THE INITIAL CONDITIONS FOR EACH CROSS-SECTION
      WRITE(108,4)
    4 FORMAT(5X'SEC-#'3X'DEPTH'4X'DISC'5X'DX'9X'MN')
      DO 6 I=1,N
      WRITE(108,5) I,Y(I,1),Q(I,1),DIST(I),MN(I)
    5 FORMAT(6X,I2,4(F9.2))
    6 CONTINUE
C
      RETURN
      END
```

```
************************************************************
C
      SUBROUTINE BREACH
C
C SUBPROGRAM TO CALCULATE THE UPSTREAM CONDITIONS OF DIS-
C CHARGE AT THE DAM SITE AS A FUNCTION OF THE RATE OF FAIL-
C URE AND THE LAKE LEVEL.
C
      COMMON/BREACHS/NUM,TSTEP,LO,L1,L2,DEPTH,BD,HDAM,
     * AREAB,FLAG,INLAKE,TQ1,VOL,MNB,TFAIL
      COMMON/PARAMETERS/Y(100,2),Q(100,2),Z(100),MN(100),
     * INFLO(100),DIST(100),QMAX(100),YMAX(100),TMAX(100),
     * XSEC(5),DT,T
      REAL LO,L1,L2,MNB,INLAKE,LDUM
      INTEGER FLAG
C
************************************************************
C
C SET TIME FACTOR
      TZERO=T
C
C LOOP THRU BREACH 'NUM' TIMES
      DO 3 I=1,NUM
C
C INCREMENT TIME COUNTER
      T = T + TSTEP
C
C PROJECT THE CHANGE IN LAKE LEVEL
      IF(I.EQ.1.AND.LO.EQ.DEPTH) DL = 0.001; GO TO 1
      DL = (LO - L1)
    1 LDUM = L1 - DL
C
C DETERMINE THE DIMENSIONS OF THE BREACH
      BD = T/(TFAIL/HDAM)
      IF(BD.GE.HDAM) BD = HDAM
      AREAB = BD**2
C
C COMPUTE THE EFFECTIVE AREA OF FLOW THRU THE BREACH
      FD = BD - (DEPTH - LDUM)
      AREAF = FD**2
C
C DETERMINE THE FRICTION SLOPE FOR THE BREACH CHANNEL
      SLOPE=((6401.9-BD+FD) - (Z(1)+Y(1,1)))/500.
C
C COMPUTE THE BREACH DISCHARGE
      BQ = 1.49/MNB * SQRT(SLOPE) * AREAF * (RADIUS(FD,
```

```
     * AREAF))**.67
C
C TOTAL DISCHARGE FROM THE DAM - SPILLWAY, OUTLET, & BREACH
      TQ2 = SPILLWAY(LDUM) + OUTLET(LDUM) + BQ
C
C COMPUTE THE NEW LAKE VOLUME AND LEVEL AFTER THE TIME STEP
      VOL = VOL + TSTEP*(INLAKE - ((TQ2+TQ1)/2.C))
      CALL LAKE(VOL,L2).
C
C TEST IF DL WAS AN APPROPRIATE PREDICTOR OF LAKE CHANGE
C IF NOT, PREDICT NEW DL AND LOOP THRU AGAIN
C OVER-ESTIMATE
      IF(L2-LDUM.GT.0.05)DL=L1-L2; OUTPUT
     * 'DL TOO LARGE'; GO TO 1
C UNDER-ESTIMATE
      IF(LDUM-L2.GT.0.05) DL=L1-L2; OUTPUT
     * 'DL TOO SMALL'; GO TO 1
C
C RE-ASSIGN VALUES FOR NEXT TIME STEP
      TQ1 = TQ2
      L0 = L1
      L1 = L2
      DT=T-TZERO
C
C OUTPUT THE BREACH HYDROGRAPH
      WRITE(101,2) T,TQ2
    2 FORMAT(2(F12.1))
    3 CONTINUE
C
C ASSIGN NEW DISCHARGE VALUE FOR NOAH
      Q(1,2) = TQ2
      OUTPUT DT,TQ2
      RETURN
      END
```

```
**********************************************************************
C
      SUBROUTINE NOAH
C
C SUBPROGRAM TO ROUTE THE FLOODWAVE DOWNSTREAM FROM THE DAM
C USING A FOUR POINT IMPLICIT FINITE DIFFERENCE METHOD FOR
C THE NUMERICAL SOLUTION OF THE COMPLETE EQUATIONS OF UN-
C STEADY FLOW.
C
      COMMON/PARAMETERS/Y(100,2),Q(100,2),Z(100),MN(100),
     * INFLO(100),DIST(100),QMAX(100),YMAX(100),TMAX(100),
     * XSEC(5),DT,T
      COMMON/ARRAY/A(200,200),N
      COMMON/CONSTANTS/G,TFINAL,THETA,NN,QTOL,YTOL
C
**********************************************************************
C
      OUTPUT'INTO NOAH'
      ITER=1; FLAG=0
C SET ARRAY TO ZERO
    1 DO 2 I=1,NN
      DO 2 J=1,NN+1
      A(I,J)=0.0
    2 CONTINUE
C
C GENERATE THE COEFFICIENT MATRIX
      OUTPUT 'INTO MATRIX...'
      CALL MATRIX
C
C SOLVE EQUATIONS SIMULTANEOUSLY
      CALL SIMEQ
C
      WRITE(108,3)
    3 FORMAT(X' X-SEC        Y1          Y2          RESY'
     *'          Q1          Q2          RESQ')
      DO 5 I=1,N
      J=(I*2)-1
C
C CORRECT THE IMPLIED DEPTHS AND DISCHARGES WITH RESIDUALS
      RESY=A(J,NN+1)
      RESQ=A(J+1,NN+1)
      Y(I,2)=Y(I,2)-RESY
      Q(I,2)=Q(I,2)-RESQ
C
C SET FLAG FOR ADDITIONAL ITERATION
      IF(ABS(RESY)-YTOL.GT.0.OR.ABS(RESQ)-QTOL.GT.0) FLAG=1
```

```
C
C OUTPUT THE RESIDUALS
      WRITE(108,4) I,Y(I,1),Y(I,2),RESY,Q(I,1),Q(I,2),RESQ
    4 FORMAT(2X,I3,6(F12.3))
    5 CONTINUE
C
C TEST FOR ADDITIONAL ITERATION
      IF(FLAG.EQ.0) GO TO 6
C
C TEST FOR CONVERGENCE
      IF(ITER.GE.25) OUTPUT'FAILS TO CONVERGE...ITER=25';
     * STOP
      ITER=ITER+1; FLAG=0; GO TO 1
C
    6 OUTPUT ITER,T,DT
      WRITE(108,7)
    7 FORMAT(X' X-SEC        Y1          Y2          Q1'
     * '        Q2')
      DO 9 I=1,N
      WRITE(108,8) I,Y(I,1),Y(I,2),Q(I,1),Q(I,2)
    8 FORMAT(2X,I3,4(F12.2))
    9 CONTINUE
C
      RETURN
      END
```

```
*****************************************************************
C
      SUBROUTINE MATRIX
C
C SUBROUTINE TO GENERATE THE MATRIX OF COEFFICIENTS FROM
C THE EQUATIONS AT EACH X SECTION AND THE UP AND DOWNSTREAM
C BOUNDARIES.
C
      COMMON/CONSTANTS/G,TFINAL,THETA,NN,QTOL,YTOL
      COMMON/PARAMETERS/Y(100,2),Q(100,2),Z(100),MN(100),
     * INFLO(100),DIST(100),QMAX(100),YMAX(100),TMAX(100),
     * XSEC(5),DT,T
      COMMON/ARRAY/A(200,200),N
      REAL INFLO,MN
C
*****************************************************************
C
C ELEMENTS OF THE MATRIX FROM THE BOUNDARY CONDITIONS
C UPSTREAM
      A(1,1)=0.0
      A(1,2)=1.0
C DOWNSTREAM
      A(NN,NN-1)=-DRCDY(Y(N,2))
      A(NN,NN)=1.0
C RESIDUALS
      A(1,NN+1)=0.0
      A(NN,NN+1)=Q(N,2)-RATING(Y(N,2))
C
      DO 1 I=1,N-1
C
C SIMPLIFY NOTATION
C
      M=2*I
      L=M-1
C
      DXDT=DIST(I)/DT
      DTDX=DT/DIST(I)
C
C DEPTHS
      Y1=Y(I,1)
      Y2=Y(I,2)
      Y3=Y(I+1,1)
      Y4=Y(I+1,2)
C
C TOP WIDTHS
      TW2=TOPW(Y2,I)
```

```
      TW4=TOPW(Y4,I+1)
C
C AREAS
      A1=AREA(Y1,I)
      A2=AREA(Y2,I)
      A3=AREA(Y3,I+1)
      A4=AREA(Y4,I+1)
C
C HYDRAULIC RADII
      R2=A2/WP(Y2,I)
      R4=A2/WP(Y4,I+1)
C
C DISCHARGES
      Q1=Q(I,1)
      Q2=Q(I,2)
      Q3=Q(I+1,1)
      Q4=Q(I+1,2)
C
C COMPUTE THE AVERAGE VALUES BETWEEN THE NODES
C
C AREAS
      AVA=(A2+A4)/2.0
C
C HYDRAULIC RADII
      AVR=(R2+R4)/2.0
C
C DISCHARGES
      AVQ=(Q2+Q4)/2.0
C
C CALCULATE THE FRICTION SLOPE TERM
      SF=(MN(I)*AVQ/AVA)**2/(2.2*AVR**1.33)
C
C COMPUTE THE DERIVATIVES OF THE FRICTION SLOPE WITH
C RESPECT TO DEPTH AND DISCHARGE
      DSFDY2=-2.0*SF*DRDY(Y2,I)/(3.0*AVR)-SF*TW2/AVA
      DSFDY4=-2.0*SF*DRDY(Y4,I+1)/(3.0*AVR)-SF*TW4/AVA
      DSFDQ2=MN(I)**2*AVQ/(2.2*AVA*AVA*AVR**1.33)
      DSFDQ4=DSFDQ2
C
C CONTINUITY EQUATION
C
C CHANGE IN Q
      DQ=(Q4-Q2)*THETA+(Q3-Q1)*(1.0-THETA)
C
C CHANGE IN Y
      DY=0.5*((Y2-Y1)+(TW4/TW2)*(Y4-Y3))
```

```
C
C RCE IS THE RESIDUAL FROM THE CONTINUITY EQUATION
      RCE=DY+DQ/(TW2*DXDT)-INFLO(I)*DT/TW2
C
C PARTIAL DERIVATIVES OF THE CONTINUITY EQUATION (CE) WITH
C RESPECT TO DEPTH AND DISCHARGE AT THE TIME LINE J+1
C
      PCEY2=0.5-(DTWDY(Y2,I)/(TW2*TW2))*(0.5*TW4*(Y4-Y3)+
     * DQ*DTDX-INFLO(I)*DT)
C
      PCEY4=0.5*TW4/TW2+0.5*DTWDY(Y4,I+1)*(Y4-Y3)/TW2
C
      PCEQ2=-DTDX*THETA/TW2
C
      PCEQ4=DTDX*THETA/TW2
C
C MOMENTUM EQUATION
C
C CHANGE IN Q WITH CHANGE IN TIME
      DQDT=-0.5*DXDT*(Q2/A2-Q1/A1+Q4/A4-Q3/A3)/G
C
C CHANGE IN Q/A WITH CHANGE IN DISTANCE (DX IS FACTORED OUT)
      DQADX=0.5*(((Q4/A4)**2-(Q2/A2)**2)/G * THETA +
     * ((Q3/A3)**2-(Q1/A1)**2)/G * (1.0-THETA))
C
C CHANGE IN ELEVATIONAL HEAD
      HEAD=THETA*(Y2+Z(I)-Y4-Z(I+1))+(1.0-THETA)*(Y1+Z(I)-
     * Y3-Z(I+1))
C
C RME IS THE RESIDUAL FROM THE MOMENTUM EQUATION
      RME=DQDT+DQADX+HEAD-(DIST(I)*SF)
C
C PARTIAL DERIVATIVES OF THE MOMENTUM EQUATION (ME) WITH
C RESPECT TO DEPTH AND DISCHARGE AT THE TIME LINE J+1
C
      PMEY2=0.5*DXDT*(Q2/A2)*(TW2/A2)/G-((Q2/A2)**2*TW2*
     * THETA)/(A2*G)+THETA-DSFDY2*DIST(I)
C
      PMEY4=0.5*DXDT*(Q4/A4)*(TW4/A4)/G+((Q4/A4)**2*TW4*
     * THETA)/(A4*G)-THETA-DSFDY4*DIST(I)
C
      PMEQ2=-0.5*DXDT/(A2*G)+(Q2/A2)*THETA/(A2*G)-DSFDQ2*
     * DIST(I)
C
      PMEQ4=-0.5*DXDT/(A4*G)-(Q4/A4)*THETA/(A4*G)-DSFDQ4*
     * DIST(I)
```

```
C
C GENERATE THE COEFFICIENT MATRIX
C
C CONTINUITY EQUATION
      A(M,L)=PCEY2
      A(M,L+1)=PCEQ2
      A(M,L+2)=PCEY4
      A(M,L+3)=PCEQ4
C MOMENTUM EQUATION
      A(M+1,L)=PMEY2
      A(M+1,L+1)=PMEQ2
      A(M+1,L+2)=PMEY4
      A(M+1,L+3)=PMEQ4
C RESIDUALS
      A(M,NN+1)=RCE
      A(M+1,NN+1)=RME
C
    1 CONTINUE
C
      RETURN
      END
```

```
*****************************************************************
C
      SUBROUTINE SIMEQ
C
C SUBROUTINE TO SOLVE THE COEFFICIENT MATRIX USING THE GAUSS
C - JORDAN ELIMINATION METHOD FOR SIMULTANEOUS EQUATIONS
C
      COMMON/ARRAY/A(200,200),N
C
*****************************************************************
C
C INITIALIZE PRGM
      NN=2*N
C
C SEARCH FOR LARGEST PIVOT ELEMENT
      DO 9 K=1,NN
      II=K
      IF(K.EQ.NN) GO TO 5
      BIG=ABS(A(K,K))
      DO 3 I=K+1,NN
      BBIG=ABS(A(I,K))
      IF(BIG.LT.BBIG) BIG=BBIG; II=I
    3 CONTINUE
C
C TEST FOR REPLACEMENT
      IF(II.EQ.K) GO TO 5
C
C SWITCHEROO
      DO 4 J=1,NN+1
      SUB=A(II,J)
      A(II,J)=A(K,J)
      A(K,J)=SUB
    4 CONTINUE
C
C CALCULATE NEW MATRIX WITHIN SAME SPACE
C (DIVIDE EQUATION BY THE LEADING COEFFICIENTS)
    5 DO 6 J=K+1,NN+1
      A(K,J)=A(K,J)/A(K,K)
    6 CONTINUE
C
C BACK SUBSTITUTION
      DO 8 I=1,NN
      IF(I.EQ.K) GO TO 8
      DO 7 J=K+1,NN+1
      A(I,J)=A(I,J)-(A(I,K)*A(K,J))
    7 CONTINUE
```

```
      8 CONTINUE
      9 CONTINUE
C
        RETURN
        END
```

```
*****************************************************************
C
      REAL FUNCTION AREA(Y,I)
C
C FUNCTION SUBROUTINE TO CALCULATE THE AREA OF FLOW AT EACH
C CROSS SECTION FROM THE DEPTH / AREA CURVES
C
      COMMON/COEFS/AC1(100),AC2(100),AC3(100),RC1,RC2,RC3
      REAL Y
      INTEGER I
C
*****************************************************************
C
      AREA = (AC1(I) * Y) + (AC2(I) * (Y**2)) + (AC3(I) *
     * (Y**3))
C
      RETURN
      END
```

```
************************************************************************
C
      REAL FUNCTION DRCDY(Y)
C
C FUNCTION SUBROUTINE TO CALCULATE THE DERIVATIVE OF THE
C DEPTH-DISCHARGE RATING CURVE (DOWNSTREAM BOUNDARY)
C
      COMMON/COEFS/AC1(100),AC2(100),AC3(100),RC1,RC2,RC3
      REAL Y
C
************************************************************************
C
      DRCDY = RC1 + 2*RC2*Y + 3*RC3*Y**2
C
      RETURN
      END
```

```
**********************************************************************
C
      REAL FUNCTION DRDY(Y,I)
C
C FUNCTION SUBROUTINE TO COMPUTE THE DERIVATIVE OF THE
C HYDRAULIC RADIUS WITH RESPECT TO DEPTH
C
      COMMON/COEFS/AC1(100),AC2(100),AC3(100),RC1,RC2,RC3
      REAL Y
      INTEGER I
C
**********************************************************************
C
      DRDY = TOPW(Y,I)/WP(Y,I)-AREA(Y,1)/(WP(Y,I)**2)*(-0.5)
     * *((TOPW(Y,I)+2.0*Y)**2)**(-1.5)*2.0*(TOPW(Y,I)+2.0*Y)
     * *(DTWDY(Y,I)+2.0)
C
      RETURN
      END
```

```
**********************************************************************
C
      REAL FUNCTION DTWDY(Y,I)
C
C FUNCTION SUBROUTINE TO COMPUTE THE DERIVATIVE OF THE TOP
C WIDTH WITH RESPECT TO DEPTH
C
      COMMON/COEFS/AC1(100),AC2(100),AC3(100),RC1,RC2,RC3
      REAL Y
      INTEGER I
C
**********************************************************************
C
      DTWDY = 2.0*AC2(I) + 6.0*AC3(I)*Y
C
      RETURN
      END
```

```
**********************************************************************
C
      SUBROUTINE LAKE(VOL,L2)
C
C FUNCTION SUBROUTINE TO CALCULATE THE LAKE DEPTH FROM THE
C DEPTH-VOLUME CURVE EQUATIONS.  THE CURVE IS TREATED AS
C TWO CURVES FOR GREATER ACCURACY.
C
      REAL VOL,L2
C
**********************************************************************
C
      IF(VOL.LE.23435280) GO TO 1
C
      L2 = (.168781E 01 + (.115480E-05 * VOL) + (-.962186
     *E-14 * (VOL**2)) + (.414551E-22 * (VOL**3)))
      RETURN
C
    1 L2 = ((.148025E-05 * VOL) + (-.267174E-13 * (VOL**2))
     * + (.309483E-21 * (VOL**3)))
C
      RETURN
      END
```

```
************************************************************************
C
      REAL FUNCTION OUTLET(Y)
C
C FUNCTION SUBROUTINE TO CALCULATE THE DISCHARGE THRU THE
C OUTLET GATES AS A FUNCTION OF LAKE LEVEL
C
      REAL Y
C
************************************************************************
C
      OUTLET = ((.350000E+01 * Y) + (-.820313E-01 * (Y**
     * 2)) + (.732422E-03 * (Y**3)))
C
      RETURN
      END
```

```
**********************************************************************
C
      REAL FUNCTION RADIUS (Y,A)
C
C FUNCTION SUBROUTINE TO CALCULATE THE HYDRAULIC RADIUS
C (R=AREA/WETTED PERIMETER)
C
      REAL Y,A
C
**********************************************************************
C
      P = SQRT(Y**2 *2.0) * 2.0
      RADIUS = A / P
C
      RETURN
      END
```

```
************************************************************************
C
      REAL FUNCTION RATING(Y)
C
C FUNCTION SUBROUTINE TO CALCULATE THE DISCHARGE AT THE
C DOWNSTREAM BOUNDARY FROM THE DEPTH-DISCHARGE RATING CURVE
C
      COMMON/COEFS/AC1(100),AC2(100),AC3(100),RC1,RC2,RC3
      REAL Y
C
************************************************************************
C
      RATING = RC1*Y + RC2*(Y**2) + RC3*(Y**3)
C
      RETURN
      END
```

```
*****************************************************************
C
      REAL FUNCTION SPILLWAY(Y)
C
C FUNCTION SUBROUTINE TO CALCULATE THE SPILLWAY DISCHARGE AS
C A FUNCTION OF LAKE DEPTH
C
      REAL Y,SD
C
*****************************************************************
C
      IF(Y.LE.42.1) SPILLWAY=0.0; RETURN
      SD = Y - 42.1
      SPILLWAY = ((.134310 E 02 * SD) + (.264744E 02 *
     * (SD**2)) + (-.107516E 01 * (SD**3)))
      RETURN
C
      END
```

```
************************************************************************
C
      REAL FUNCTION TOPW(Y,I)
C
C FUNCTION SUBROUTINE TO CALCULATE THE TOP WIDTH OF FLOW AT
C EACH CROSS-SECTION AS THE DERIVATIVE OF THE AREA WITH
C RESPECT TO DEPTH)
C
      COMMON/COEFS/AC1(100),AC2(100),AC3(100),RC1,RC2,RC3
      REAL Y
      INTEGER I
C
************************************************************************
C
      TOPW = AC1(I) + 2*AC2(I)*Y + 3*AC3(I)*Y**2
C
      RETURN
      END
```

```
************************************************************************
C
      REAL FUNCTION VOLUME(Y)
C
C FUNCTION SUBROUTINE TO CALCULATE THE INITIAL VOLUME OF THE
C LAKE FROM THE DEPTH-VOLUME CURVE.  THE CURVE IS BROKEN
C INTO TWO SECTIONS AND TREATED WITH TWO EQUATIONS FOR IN-
C CREASED ACCURACY.
C
      REAL Y
C
************************************************************************
C
      IF(DEPTH.LE.24) GO TO 1
C
      VOLUME = -.232320E 06 + (.791340E 06 * Y) +
     * (.388208E 04 * (Y**2)) + (.176458E 03 * (Y**3))
      RETURN
C
    1 VOLUME = (.674273E 06 * Y) + (.816750E 04 * (Y**2)) +
     * (.184336E 03 * (Y**3))
C
      RETURN
      END
```

```
**********************************************************************
C
      REAL FUNCTION WP(Y,I)
C
C FUNCTION SUBROUTINE TO CALCULATE THE WETTED PERIMETER AT
C EACH X-SECTION AS A FUNCTION OF THE DEPTH
C
      COMMON/COEFS/AC1(100),AC2(100),AC3(100),RC1,RC2,RC3
      REAL Y
      INTEGER I
C
**********************************************************************
C
      WP = SQRT(TOPW(Y,I)**2 + Y**2) + Y
C
      RETURN
      END
```

APPENDIX III
EXAMPLE DATA FILE

```
DEPTH INLAKE TSTEP   MNB    TFAIL
 48    1000   5.0   0.047  450.
 N TFINAL THETA QTOL YTOL
97 3600.0  0.6  50.0  .05
20,50,70,97      X-SECTIONS FOR HYDROGRAPHS (1=DAMSITE)
 Z(I)    DIST(I) INFLO(I)      X-SEC=I (NOT READ IN)
 6330.0  100.0     .0             1
 6310.0  100.0     .0             2
 6290.0  125.0     .0             3
 6265.0  125.0     .0             4
 6244.2  150.0     .0             5
 6226.6  150.0     .0             6
 6210.3  175.0     .0             7
 6198.0  175.0     .0             8
 6185.8  200.0     .0             9
 6175.6  200.0     .0             10
 6166.0  225.0     .0             11
 6155.1  225.0     .0             12
 6144.3  250.0     .0             13
 6132.2  250.0     .0             14
 6120.2  275.0     .0             15
 6109.7  275.0     .0             16
 6102.3  300.0     .0             17
 6093.6  300.0     .0             18
 6084.9  325.0     .0             19
 6075.6  325.0     .0             20
 6066.7  350.0     .0             21
 6057.3  350.0     .0             22
 6049.6  375.0     .0             23
 6042.3  375.0     .0             24
 6035.0  400.0     .0             25
 6027.2  400.0     .0             26
 6019.4  425.0     .0             27
 6011.2  425.0     .0             28
 6002.9  450.0     .0             29
 5994.1  450.0     .0             30
 5985.4  475.0     .0             31
 5976.1  475.0     .0             32
 5966.9  500.0     .0             33
 5953.9  500.0     .0             34
 5938.9  525.0     .0             35
 5924.4  550.0     .0             36
 5909.2  550.0     .0             37
 5894.1  575.0     .0             38
```

5878.2	575.0	.0	39
5862.3	600.0	.0	40
5845.7	600.0	.0	41
5829.2	625.0	.0	42
5811.9	625.0	.0	43
5797.3	650.0	.0	44
5784.8	650.0	.0	45
5772.4	675.0	.0	46
5759.5	675.0	.0	47
5746.6	700.0	.0	48
5733.2	700.0	.0	49
5718.8	725.0	.0	50
5703.2	725.0	.0	51
5687.5	750.0	.0	52
5671.0	750.0	.0	53
5654.1	775.0	.0	54
5636.7	775.0	.0	55
5619.3	800.0	.0	56
5601.3	800.0	.0	57
5581.6	825.0	.0	58
5558.6	825.0	.0	59
5535.5	850.0	.0	60
5511.8	850.0	.0	61
5488.1	875.0	.0	62
5463.6	875.0	.0	63
5439.2	900.0	.0	64
5414.0	900.0	.0	65
5391.1	925.0	.0	66
5368.7	925.0	.0	67
5346.3	950.0	.0	68
5324.9	950.0	.0	69
5305.7	975.0	.0	70
5286.1	975.0	.0	71
5267.1	1000.0	.0	72
5247.6	1000.0	.0	73
5230.2	1025.0	.0	74
5217.1	1025.0	.0	75
5204.0	1050.0	.0	76
5190.6	1050.0	.0	77
5177.2	1075.0	.0	78
5163.4	1075.0	.0	79
5145.9	1100.0	.0	80
5127.3	1100.0	.0	81
5110.1	1125.0	.0	82
5093.8	1125.0	.0	83
5075.1	1150.0	.0	84

5049.5	1150.0	.0	85
5030.7	1175.0	.0	86
5013.4	1175.0	.0	87
4997.5	1200.0	.0	88
4982.1	1200.0	.0	89
4965.9	1225.0	.0	90
4948.4	1225.0	.0	91
4931.1	1250.0	.0	92
4913.8	1250.0	.0	93
4897.0	1275.0	.0	94
4881.3	1275.0	.0	95
4865.6	875.0	.0	96
4855.1	0.0	.0	97

.242019E+03	-.131602E+03	.217446E+02	RATING-CURVE Q
-.246667E+01	.598750E+01	-.490833E-01	1
.118736E+02	.374275E+01	.112385E-01	2
.262140E+02	.149800E+01	.715603E-01	3
.441394E+02	-.130794E+01	.146963E+00	4
.495098E+02	-.981685E+00	.139565E+00	5
.333553E+02	.504776E+01	-.183523E-01	6
.175051E+02	.983465E+01	-.144254E+00	7
.787849E+00	.817113E+01	-.104385E+00	8
-.159294E+02	.650762E+01	-.645164E-01	9
-.127807E+02	.613183E+01	-.556568E-01	10
-.645286E+01	.597395E+01	-.520408E-01	11
.665988E+00	.579634E+01	-.479729E-01	12
.778483E+01	.561873E+01	-.439049E-01	13
.156947E+02	.542138E+01	-.393849E-01	14
.236045E+02	.522404E+01	-.348649E-01	15
.331101E+02	.201692E+01	.589827E-01	16
.428910E+02	-.414576E+01	.256948E+00	17
.428749E+02	-.359250E+01	.387977E+00	18
.270954E+02	-.115713E+01	.232514E+00	19
.100009E+02	.148120E+01	.640953E-01	20
.279490E+01	.351339E+01	.593977E-01	21
.169035E+01	.529394E+01	.164535E+00	22
-.108028E+00	.615150E+01	.189312E+00	23
-.244786E+01	.652092E+01	.168025E+00	24
-.478769E+01	.689034E+01	.146739E+00	25
-.728351E+01	.728439E+01	.124033E+00	26
-.977933E+01	.767844E+01	.101327E+00	27
-.124311E+02	.809712E+01	.772021E-01	28
-.150829E+02	.851579E+01	.530772E-01	29
-.178907E+02	.895910E+01	.275332E-01	30
-.206985E+02	.940240E+01	.198921E-02	31
-.236623E+02	.987034E+01	-.249739E-01	32

-.266261E+02	.103383E+02	-.519370E-01	33
-.167960E+02	.721348E+01	-.384399E-01	34
-.108167E+01	.267432E+01	-.528044E-02	35
-.937800E+00	.384151E+01	-.195932E-01	36
-.787081E+00	.506428E+01	-.345876E-01	37
-.636362E+00	.628705E+01	-.495819E-01	38
-.478792E+00	.756541E+01	-.652579E-01	39
-.321222E+00	.884376E+01	-.809338E-01	40
-.156802E+00	.101777E+02	-.972914E-01	41
.761916E-02	.115116E+02	-.113649E+00	42
.178891E+00	.129011E+02	-.130688E+00	43
.116312E+01	.128073E+02	-.129649E+00	44
.310264E+01	.110385E+02	-.108200E+00	45
.504216E+01	.926973E+01	-.867512E-01	46
.705628E+01	.743290E+01	-.644775E-01	47
.907040E+01	.559608E+01	-.422037E-01	48
.111591E+02	.369122E+01	-.191050E-01	49
-.579798E+01	.696718E+01	-.497944E-01	50
-.361247E+02	.138322E+02	-.117628E+00	51
-.664513E+02	.206971E+02	-.185461E+00	52
-.709898E+02	.219970E+02	-.197445E+00	53
-.520487E+02	.182201E+02	-.158514E+00	54
-.324763E+02	.143173E+02	-.118285E+00	55
-.129039E+02	.104145E+02	-.780559E-01	56
.729996E+01	.638586E+01	-.365293E-01	57
.190207E+02	.376349E+01	-.100859E-01	58
.165269E+02	.347608E+01	-.874091E-02	59
.140331E+02	.318867E+01	-.739592E-02	60
.114638E+02	.289256E+01	-.601016E-02	61
.889446E+01	.259644E+01	-.462441E-02	62
.624956E+01	.229161E+01	-.319790E-02	63
.360466E+01	.198679E+01	-.177138E-02	64
.884193E+00	.167325E+01	-.304110E-03	65
.119896E+02	.314149E+01	-.153541E-01	66
.314351E+02	.568554E+01	-.404174E-01	67
.508805E+02	.822960E+01	-.654807E-01	68
.557764E+02	.877772E+01	-.712899E-01	69
.399437E+02	.648686E+01	-.496933E-01	70
.297665E+02	.518734E+01	-.375992E-01	71
.431190E+02	.796284E+01	-.645299E-01	72
.568139E+02	.108095E+02	-.921513E-01	73
-.108824E+03	.551594E+02	-.180467E+01	74
-.707507E+03	.199880E+03	-.758972E+01	75
-.130619E+04	.344600E+03	-.133748E+02	76
-.191947E+04	.492850E+03	-.193010E+02	77
-.253276E+04	.641100E+03	-.252272E+02	78

-.316065E+04	.792879E+03	-.312944E+02	79
-.205145E+04	.504827E+03	-.179111E+02	80
-.570831E+03	.122561E+03	-.346508E+00	81
.167609E+03	-.719081E+02	.921598E+01	82
.290291E+03	-.110744E+03	.121757E+02	83
.245549E+03	-.962012E+02	.118241E+02	84
-.270836E+03	.687155E+02	.215609E+01	85
-.409144E+03	.132961E+03	-.118251E+01	86
-.443155E+03	.170031E+03	-.279732E+01	87
-.177648E+04	.503607E+03	-.183009E+02	88
-.389012E+04	.101588E+04	-.421722E+02	89
-.421597E+04	.107702E+04	-.440791E+02	90
-.199358E+04	.494706E+03	-.146351E+02	91
-.433116E+03	.852507E+02	.543648E+01	92
-.233915E+03	.312371E+02	.619228E+01	93
.156759E+03	-.623426E+02	.797832E+01	94
-.153337E+03	.362106E+02	.297357E+01	95
-.839801E+02	.144827E+02	.560922E+01	96
-.454163E+02	-.419500E+01	.648205E+01	97